National Library of Canada
Acquisitions and Bibliographic Services Branch
395 Wellington Street
Ottawa, Ontario
K1A 0N4

Bibliothèque nationale du Canada
Direction des acquisitions et des services bibliographiques
395, rue Wellington
Ottawa (Ontario)
K1A 0N4

Your file Votre référence

Our file Notre référence

NOTICE

The quality of this microform is heavily dependent upon the quality of the original thesis submitted for microfilming. Every effort has been made to ensure the highest quality of reproduction possible.

If pages are missing, contact the university which granted the degree.

Some pages may have indistinct print especially if the original pages were typed with a poor typewriter ribbon or if the university sent us an inferior photocopy.

AVIS

La qualité de cette microforme dépend grandement de la qualité de la thèse soumise au microfilmage. Nous avons tout fait pour assurer une qualité supérieure de reproduction.

S'il manque des pages, veuillez communiquer avec l'université qui a conféré le grade.

La qualité d'impression de certaines pages peut laisser à désirer, surtout si les pages originales ont été dactylographiées à l'aide d'un ruban usé ou si l'université nous a fait parvenir une photocopie de qualité inférieure.

Canada

BUFFETING ANALYSIS OF CABLE-STAYED BRIDGES DURING THEIR ERECTION

BY

ZHONG YING HUANG

Thesis submitted to the University of Ottawa
as a partial fulfilment of the requirements
for the Master of Applied Science
Department of Civil Engineering
University of Ottawa

April 1995

National Library
of Canada

Acquisitions and
Bibliographic Services Branch

395 Wellington Street
Ottawa, Ontario
K1A 0N4

Bibliothèque nationale
du Canada

Direction des acquisitions et
des services bibliographiques

395, rue Wellington
Ottawa (Ontario)
K1A 0N4

Your file Votre référence

Our file Notre référence

ISBN 0-612-07799-3

Canada

UNIVERSITÉ D'OTTAWA
UNIVERSITY OF OTTAWA

Abstract

Buffeting response of cable-stayed bridges at their erection stage under yawed wind has attracted engineering attention through wind tunnel observations and studies. Cable-stayed bridges are particularly vulnerable to dynamic wind effects during their construction stages due to the lack of overall structural stiffness. The most critical stage is just before the bridge main span is closed. At this time, a cable-stayed bridge resembles a long cantilever structure supported by cables, and particularly, the fundamental frequency in horizontal modes of oscillation may be very low. During this stage, the cable-stayed bridge is more responsive to wind action both in lateral and vertical bending. For this reason, the prediction of wind-induced bridge response becomes more important when directional variation of wind is considered. However, only a few theoretical approaches have been proposed, applicable only in extremely simplified cases.

This thesis deals with the prediction of buffeting response of cable-stayed bridges under yawed winds using the modified buffeting analysis. The modified buffeting analysis was originally developed by Kimura(1991) and was restricted to vertical bending response. The comparison with experimental data was also conducted for extremely simplified flat plate models. In this thesis, the modified buffeting approach is not only applied to actual cable-stayed bridge models but also the calculation of the lateral bending oscillation has been attempted. Further, the calculated results are compared with the experimental data obtained from the wind tunnel tests of the aeroelastic cable-stayed bridge models; the Normandy Bridge and the Kao Ping Hsi Bridge.

Acknowledgement

The author would like to express her deepest gratitude to her research supervisor, Dr. H. Tanaka for his guidance and encouragement throughout the period of this study.

Thanks is also extended to Dr. K. Kimura, the University of Tokyo, Japan, for his personal communications and helpful advice. The author also appreciates access to the experimental data and related information given to her from the Danish Maritime Institute, Denmark.

The author gratefully acknowledges the financial support provided by The Natural Science and Engineering Research Council through her research supervisor, The University of Ottawa scholarship and also by the author's parents.

Table of Contents

Notation

The following symbols are used in this thesis.

. **Small letters**

c	coherence coefficient or decay factor
f	frequency
l	length
m	distributed mass per unit length
q	generalized coordinate
rms	root-mean-square or standard deviation
t	time
u,v,w	fluctuating wind velocity component
x,y,z	coordinates

. **Capital letters**

A	area
Ai*	flutter derivative
AR	aspect ratio
B	deck width
C_D	drag coefficient
C_L	lift coefficient
C_M	moment coefficient
C_N	normal force coefficient
C_x	lateral force coefficient
C_z	vertical force coefficient
$C_{L\alpha}$	lift slope
D	drag force

F_x, F_z	aerodynamic force components in x,z-direction
H_i^*	flutter derivative
$\| H(f) \|^2$	mechanical admittance
I_u, I_w	turbulence intensities
K	reduced frequency
L	lift force per unit span
L_u, L_w	turbulence length scales
M	aerodynamic pitching moment
M_i	generalized mass for the i-mode
P_i^*	flutter derivative
R	coherence function
S	power spectrum
S_F	force spectra
S_u,S_v,S_w	velocity spectra of u,v,w-component
S_{uu}, S_{ww}	cross spectra of u,w-component
U	mean weed speed
U_r	relative wind velocity
U_c,U_s	effective wind speed of the cosine and sine case
Z	height

. **Greek letters**

α	angle of attack
β	wind yaw angle
θ	torsional displacement
ζ_s	structural damping ratio
ζ_a	aerodynamic damping ratio
ρ	air density
σ	rms response

Φ	mode shape
ω	circular frequency

Chapter 1
Introduction

1.1 A Brief Survey of Bridge Aerodynamics

All suspended bridges are susceptible to wind-induced problems. Historically, there have been records that many suspension bridges were either destroyed or severely damaged by wind action. However, the dynamic response of bridges caused by wind action has never attracted much concern until the dramatic collapse of the Tacoma Narrows Bridge in 1940. After this disaster, more scientific attention and investigation have been devoted to problems of bridge aerodynamics.

The early aerodynamic investigations were made mainly by Farquharson et al [13] and Scruton [36]. Their research focussed attention on the importance of dynamic effects of wind and provided a solid foundation for subsequent research and development of bridge aerodynamics. A significant contribution was model testing, section models and full bridge models, in conventional aeronautical wind tunnels with smooth uniform flow.

In the early 1960's, Davenport (1962) pointed out the importance of considering natural wind conditions for bridge response. For the first time, wind was considered as an atmospheric boundary layer flow with three-dimensional structure of the turbulence. Since then, many experiments of full bridge models have been conducted in wind tunnels with simulated natural wind [5,9,25,28,54,55].

At present, the experimental studies for the aerodynamic performance of bridges under wind action are still important procedures. The wind tunnel testing techniques for bridge models can be classified by model types which are; section models, full models and taut strip models; or by the flow conditions which are smooth or turbulent. Each technique

has its own special advantages and disadvantages [57].

There are many analytical approaches for predicting dynamic response of bridges including the buffeting analysis proposed by Davenport [6] based on the quasi-steady assumption, and the bridge flutter theory developed by Scanlan [30] in terms of the aerodynamic derivatives determined experimentally in wind tunnel using two-dimensional or sectional models.

In both experimental and theoretical means, the understanding of bridge aerodynamics has progressed quite significantly in the last half century. At the same time, development in bridge design and construction has progressed. An obvious example is the development of cable-stayed bridges. Since the first modern cable-stayed bridge was built in Sweden in 1955, cable-stayed bridges have become very popular and spread rapidly throughout the world. In particular, the growth of span length is remarkable in the past decade, which leads to more complicated aerodynamic behaviour. It is therefore very important to consider and investigate carefully the dynamic properties of cable-stayed bridges , not only for completed bridges, but for bridges in the construction stage as well.

1.2 Wind Induced Dynamic Behaviour of Cable-Stayed Bridges

With increasing popularity, cable-stayed bridges have now been constructed throughout the world. The recent trend of longer-span cable-stayed bridges is quite remarkable. For example, the Normandy Bridge (France) with a main span of 856 m, and the Tatara Bridge (Japan) with a centre span of 890 m are currently under construction [26].

However, a long-span cable-stayed bridge design results in a more flexible structural system, making the dynamic behaviour more complicated. It has become very important for the design of cable-stayed bridges to consider dynamic effects caused by wind induced vibration.

Wind effects on long-span bridge are generally classified into two groups ; i. e. static and dynamic behaviours [43] as follows :

(1) Static behaviours
    . Overturning
    . Excessive lateral deflection
    . Divergence
    . Lateral buckling

(2) Dynamic behaviours
    . Vortex induced oscillation
    . Self-excited oscillation
        . Vertical bending instability
        . Torsional instability
        . Coupled flutter
    . Buffeting motion

Static phenomena have been well accepted and can be predicted by theoretical calculations with good accuracy as long as the aerodynamic force components, lift and drag forces and pitching moment are known. The following discussion is mainly on dynamic phenomena.

Vortex Induced Oscillation

Vortex induced oscillation is an aerodynamic phenomenon. When air flow comes to a bridge structure, a periodic vortex shed tends to be formed in its wake. The periodic shedding of vortices alternately from the upper and lower surfaces of the bridge causes periodic fluctuation of the aerodynamic lift forces on the bridge. Since the vortex shedding frequency is basically proportional to the wind speed, it can coincide with or become very close to a natural frequency of the bridge. Once the structural motion is induced by this resonating effect, the shedding frequency, in turn, can be controlled by the structural motion. This leads to a more complicated flow-structure interaction phenomena which can

sustain the vibration for a while. The amplitude of oscillation will depend on the level of structural damping and the geometric shape of the deck cross-section. The response can be characterized as a nonlinear limit cycle type phenomenon.

Self-Excited Oscillations

Self-excited oscillations are caused by additional forces which depend on the motion of the structure itself and can be described as unstable oscillations. The vertical bending instability and torsional instability are considered to be the single-degree-of-freedom flutters associated with the negative aerodynamic damping forces. Coupled flutter (or classical flutter) is a combined oscillation of torsional and vertical bending modes. Scanlan formulated the flutter of bridge decks [4] following the formulation of wing flutter and introduced the dimensionless aerodynamic derivatives determined by wind tunnel tests of section models.

Buffeting Motion

Buffeting is defined as a randomly forced vibration of a structure due to velocity fluctuations in the oncoming flow. The buffeting forces are usually assumed to be random functions only of time and spatial location, i.e. not interactive with structural motion. It means that the buffeting motion is considered to be a pure forced vibration. The buffeting effect is a vitally important factor to be considered in the design of cable-stayed bridges.

The aerodynamic phenomena caused by wind induced oscillation have been briefly described above. These aerodynamic phenomena must be considered in the design of long, flexible bridges. Also, it should be seen that not all phenomena are equally likely to occur, and certainly not all phenomena lead to catastrophic failures.

Vortex shedding induced vibrations commonly occur for pipeline suspension bridges, and components (such as hangers and cables) on other bridges [57]. The vortex-induced

oscillation is a serious matter in the case of resonance-excitation, which appears at a certain wind velocity, and causes vibration with limited amplitudes; The self-excited oscillations are the most dangerous aerodynamic phenomena which appear at or above the critical wind velocity and cause divergent amplitude response until the structure collapses. The failure to prevent major oscillations is usually catastrophic. Aerodynamic instabilities have occurred with some suspension bridges in the past such as the case of the Tacoma Narrows Bridge. Though there have not been any observed instabilities with cable-stayed bridges until today, it is still important that critical wind velocities for the self-excited oscillations should be beyond the realistic range of wind speeds.

Buffeting motion can occur in any bridges due to the atmospheric turbulence. The dynamic response may increase at higher wind speeds. Though buffeting effects may not cause collapse of the bridge immediately, it could cause fatigue damage of structural materials or problems in the serviceability of the bridge. The essential purpose of buffeting analysis for long span bridges is to ensure the reliability of the structures under turbulent wind.

For a completed bridge, buffeting becomes important at high wind speeds. However, for cable-stayed bridges, serious buffeting motion may occur during their erection at wind speeds below the design wind speed for the completed bridge. In particular, when a cable-stayed bridge is under construction during its final stage but the deck has not been closed at the span centre, it resembles a half-span cantilever structure and the natural frequencies may be very low both in lateral and vertical bending oscillations. Buffeting response to gusts is then a serious issue. There have been several experimental observations and investigations of cable-stayed bridges [5,24,25] which have shown even higher response under winds horizontally skewed from normal to the bridge axis. The yawed wind effect is thus an important consideration for cable-stayed bridges during their erection. For this reason, this thesis focusses on the buffeting response of cable-stayed bridges during their erection, and the directional variation of wind is also considered.

Though there have been a few analytical attempts to investigate this problem, they have covered only extremely simplified cases. The subject of this thesis is to further develop the modified buffeting approach and predict the buffeting response for actual cable-stayed bridges during their erection. Also, the analytical results are compared with the experimental data measured through wind tunnel tests.

1.3 Objective and Scope of the Thesis

The objective of the thesis is to extend the original modified buffeting approach to include prediction of lateral buffeting response. Also a computer programme was designed and applied to both vertical and lateral buffeting prediction of actual cable-stayed bridges. Finally the analytical results are compared with experimental results.

The scope of the thesis is as follows:

Chapter 1 presents a brief survey of the development of bridge aerodynamics and the wind-induced dynamic behaviours of cable-stayed bridges.

Chapter 2 focusses on buffeting motion of cable-stayed bridges. First, the conventional buffeting analytical procedure is described, which considers only winds normal to the bridge span. Then the effects of yawed wind on cable-stayed bridges under construction are discussed, and a summary of some experimental evidence and a few analytical approaches are presented. Further, the modified buffeting analysis applicable to vertical response proposed by Kimura [24] is explained. Finally, the author extends the approach to predict lateral bending oscillation of cable-stayed bridges.

Chapter 3 presents the analytical prediction of buffeting both in lateral and vertical bending oscillations for the aeroelastic cable-stayed bridge models of the Normandy Bridge and the Kao Ping Hsi Bridge, and compares them with the experimental results.

Chapter 4 describes some discussions on effects of aerodynamic parameters on wind induced buffeting response of bridges.

Brief concluding remarks and suggested further study are given in Chapter 5.

Chapter 2
Theoretical Analysis of Bridge Buffeting Response

2.1 Introduction

The buffeting response of a cable-stayed bridge is usually caused by wind turbulence. The response can be one or a combination of more than one random vibrations in lateral bending, vertical bending or torsion around the longitudinal axis of a bridge deck . At high wind speeds, the buffeting of the bridge deck becomes an element for design consideration of cable-stayed bridges. The magnitude of a bridge buffeting response not only depends on the wind speed, the geometrical shape of the bridge deck, the structural damping and natural frequencies of the bridge, but also on the properties of wind turbulence, such as turbulence intensities, the length scales of turbulence and the energy spectra of turbulence components.

Usually, the conventional buffeting analysis investigates only winds normal to the bridge span. However, some wind tunnel observations and studies have indicated that an even higher response may occur in winds with skew angles. Moreover, it would certainly be necessary to consider winds from all directions for the calculation of peak response probability of the bridge for any return period. This can only be assessed if the effect of wind directions on buffeting response is known.

In this section, the development of research on buffeting analysis is briefly surveyed and the typical procedures for the conventional buffeting theory are reviewed. The effects of yaw angles on cable-stayed bridges are then discussed. Finally, the modified buffeting approach in prediction of both lateral and vertical buffeting is explained.

2.2 Prediction of Buffeting Response

The prediction of the buffeting response to turbulent wind is a statistical approach based on the concepts of power spectra to describe stochastic loads of stationary random series and the statistical properties of the turbulence. In other words, the mathematical analysis of buffeting is based on the theory of random vibration which predicts the root-mean square (rms) response of structures through a frequency domain analysis. It is accomplished by relating the frequency components of aerodynamic forces and those of the structural response by considering the structure's sensitivity to each frequency given by the frequency response function. The theoretical approach applied to civil engineering structures of line-like form, such as long-span bridges, tall masts and overhead power lines, was first developed by Davenport [6], which is based on the following assumptions:

(1) The most serious effects are likely to occur under winds normal to the longitudinal axis of the structure;

(2) Small changes of wind direction in the direction of the axis of the structure have little or no effect on the loading;

(3) Because the structures are sufficiently slender, only the two-dimensional flow condition can be applied to each span-wise segment;

(4) The turbulent fluctuations are so small when compared to the mean velocity that the gust loading can be expressed as linear functions of the gust velocity.

The third assumption is also called the strip theory approximation, which indicates that the aerodynamic forces acting on a section only depend on the flow pattern determined by the cross-section and the angle of attack.

Another widely used assumption is the quasi-steady aerodynamic assumption which summarizes that the instantaneous forces acting on a structure are taken equal to the steady forces induced by a steady wind having the same relative velocity and direction as the instantaneous wind. With this approximation, the aerodynamic forces at any instant depend

on the relative wind speed at that instance, and they are given in terms of parameters that must be determined experimentally. This approach has been shown to be valid, especially for small reduced frequency fB/U (or large reduced velocity), where U is the mean wind speed, f is the natural frequency of the flow fluctuation and B is the width of the structure. When the reduced frequency is very small, the flow around the structure is regarded as steady state. However, for large structures such as long-span bridges, the effect of non-uniform flow around their cross-section should be considered. The aerodynamic admittance is introduced as a correction factor for the quasi-steady approximation, and it is considered to be a transfer function from fluctuating wind velocity power spectra to the aerodynamic loading power spectra of the section in the frequency domain.

The theoretical approach, known as the conventional buffeting theory or the quasi-steady aerodynamic approach, is now most widely used for predicting the buffeting response of long-span bridges by applying experimental data obtained from section model tests. However, this buffeting theory is limited to cases of the wind normal to the bridge axis.

2.2.1 Aerodynamic Forces

Consider a bridge deck section and let x, z and θ be the horizontal, vertical and torsional displacement of the bridge deck section, respectively , as illustrated in Fig. 2.1. When the bridge deck is buffeted by turbulent wind, the aerodynamic forces acting on the bridge deck are aerodynamic drag, lift and moment. Usually the aerodynamic behaviour of the structure may be assumed to be linear; i.e. the aerodynamic forces can be expressed as a linear combination of the forces caused by the movement in each degree of freedom and the linear buffeting forces induced by the velocity fluctuation of the incident flow.

The aerodynamic forces per unit length of the bridge in its span direction may be written in forms based on the linear assumption as follows:

$$\text{Lift force} = L_{se} + L_b \tag{2.1}$$

$$\text{Drag force} = D_{se} + D_b \tag{2.2}$$

$$\text{Moment} = M_{se} + M_b \tag{2.3}$$

where Lse, Dse and Mse refer to the self-excited force components of aerodynamic lift, drag and moment; Lb , Db and Mb are aerodynamic forces due to buffeting effects. Ref. [4] offers the expressions of self-excited aerodynamic forces and buffeting forces as follows:

$$L_{se} = 0.5\rho U^2 B \left[KH_1^*(K) (\dot{z} / U) + KH_2^*(K) (B \dot{\theta} /U) + K^2 H_3^*(K)\theta \right] \tag{2.4}$$

$$D_{se} = 0.5\rho U^2 B \left[KP_1^*(K) (\dot{x} / U) + KP_2^*(K) (B \dot{\theta} /U) + K^2 P_3^*(k)\theta \right] \tag{2.5}$$

$$M_{se} = 0.5\rho U^2 B^2 \left[KA_1^*(K) (\dot{z} /U) + KA_2^*(K) (B \dot{\theta} /U) + K^2 A_3^*(K)\theta \right] \tag{2.6}$$

where: ρ = air density;

U = mean wind speed;

B = bridge deck width;

K = reduced frequency which is defined as $K = B\omega/U$;

ω = circular frequency;

$H_i^*(K)$, $P_i^*(K)$ and $A_i^*(K)$ (i=1,2,3) are flutter derivatives which are obtained experimentally.

The sectional buffeting lift, drag and moment forces are expressed in terms of steady average lift, drag and twist force coefficients C_L, C_D and C_M respectively,

$$L_b = 0.5\ \rho U^2 B \{ C_L (1 + 2\, u(t) /U) + (C_L' + C_D)\, w(t)/U \} \tag{2.7}$$

$$D_b = 0.5\ \rho\ U^2\ B \{ C_D (1 + 2\, u(t) /U) + C_D'\, w(t) / U \} \tag{2.8}$$

$$M_b = 0.5\ \rho\ U^2\ B^2 \{ C_M (1 + 2\, u(t) /U) + C_M'\, w(t) / U \} \tag{2.9}$$

where u(t) and w(t) are the along-wind and vertical gust velocity components respectively; $C_L' = dC_L/d\alpha$, $C_D' = dC_D/d\alpha$, and $C_M' = dC_M/d\alpha$.

Equations (2.7) - (2.9) are based on the assumption that the fluctuation of the buffeting forces is proportional only to that of u(t) and w(t). By taking the fluctuating parts of (2.7) to (2.9), the aerodynamic buffeting forces may be expressed as:

$$F_{Lb}(t) = 0.5\rho\, U^2 B \{ 2u(t) C_L /U + (C_L' + C_D) w(t) /U \} \qquad (2.10)$$

$$F_{Db}(t) = 0.5\rho\, U^2 B \{ 2w(t) C_D /U + C_D' w(t) /U \} \qquad (2.11)$$

$$F_{Mb}(t) = 0.5\rho\, U^2 B^2 \{ 2u(t) C_M/U + C_M' w(t) / U \} \qquad (2.12)$$

Equations (2.10) - (2.12) are expressions of aerodynamic buffeting forces caused by u(t) and w(t) components of fluctuating velocities.

Furthermore, when the quasi-steady theory is used, the aerodynamic forces acting on a bridge deck are buffeting forces given in (2.10) - (2.12) and aerodynamic damping forces. Aerodynamic damping forces are important in estimating the level of damping provided by the motion-induced forces on the bridge deck. Fig. 2.2 represents the aerodynamic damping forces caused by the motion of the deck, in which α is the angle of attack, and U_r is the relative wind speed.

When the deck moves under a horizontal wind, the velocity of the wind relative to the moving deck can be expressed as:

$$U_r^2 = (U + \dot{x})^2 + \dot{z}^2 \qquad (2.13)$$

Because only horizontal and vertical responses are considered in the present analysis, the aerodynamic drag and lift forces are defined as $D(\alpha)$ and $L(\alpha)$ which are functions of the angle of attack α, and they can be written as:

$$D(\alpha) = 0.5\rho\, BU_r^2\, C_D(\alpha) \tag{2.14}$$

$$L(\alpha) = 0.5\rho\, BU_r^2\, C_L(\alpha) \tag{2.15}$$

where $C_D(\alpha)$ and $C_L(\alpha)$ are drag and lift coefficients with a small angle of wind incidence. The horizontal and vertical forces per unit length due to deck motion can be expressed as:

$$F_x = -D(\alpha)\cos\alpha + L(\alpha)\sin\alpha \tag{2.16}$$

$$F_z = -D(\alpha)\sin\alpha - L(\alpha)\cos\alpha \tag{2.17}$$

Substituting equations (2.13), (2.14) and (2.15) to (2.16) and (2.17), and assuming a small amplitude motion, i.e. the terms involving the products of x and z can be neglected. The force equations become:

$$F_x = 0.5\rho\, B\,(U^2 + 2U\dot{x})\,[-C_D(\alpha)\cos\alpha + C_L(\alpha)\sin\alpha] \tag{2.18}$$

$$F_z = -0.5\rho B\,(U^2 + 2U\dot{x})\,[C_D(\alpha)\sin\alpha + C_L(\alpha)\cos\alpha] \tag{2.19}$$

letting

$$C_x(\alpha) = -C_D(\alpha)\cos\alpha + C_L(\alpha)\sin\alpha \tag{2.20}$$

$$C_z(\alpha) = -C_D(\alpha)\sin\alpha - C_L(\alpha)\cos\alpha \tag{2.21}$$

F_x and F_z can be expressed as:

$$F_x = 0.5\rho\, B\,[U^2 + 2U\dot{x}]\,C_x(\alpha) \tag{2.22}$$

$$F_z = 0.5\rho\, B\,[U^2 + 2U\dot{x}]\,C_z(\alpha) \tag{2.23}$$

in the equation (2.22), the first term represents the mean wind load and the second term is the aerodynamic damping in horizontal direction. If the bridge deck has mass m per unit length, stiffness and linear mechanical damping, the equation of motion in horizontal direction can be written in the usual form:

$$m\left(\ddot{x} + 2\,\zeta_s\,\omega_x\,\dot{x} + \omega_x^{\,2}\,x\right) = F_x \tag{2.24}$$

where ω_x is a circular frequency in horizontal direction. By substituting (2.22) to (2.24), and combining the damping terms, the aerodynamic damping ratio can be expressed as:

$$\zeta_{ax}(\alpha) = -\frac{\rho U B}{2m\omega_x} C_x(\alpha) \tag{2.25}$$

Usually the angle of attack α is very small. If $\alpha \doteq 0$, the equation (2.25) can be approximated as:

$$\zeta_{ax} = \frac{\rho U B}{2m\omega_x} C_D \tag{2.26}$$

where $\zeta_{ax} = \zeta_{ax}(0)$, and $C_D = C_D(0)$.

The equation (2.26) gives aerodynamic damping ratio in lateral oscillation based on the quasi-steady assumption.

In order to obtain the aerodynamic damping force in vertical direction for a small motion, the force can be approximated as:

$$F_z = \frac{\partial F_z}{\partial \alpha}\bigg|_{\alpha=0} \alpha \tag{2.27}$$

using (2.23)

$$\frac{\partial F_z}{\partial \alpha} = 0.5\rho B\,(U^2 + 2U\dot{x})\,\frac{\partial C_z(\alpha)}{\partial \alpha}$$

$$= -0.5\rho B(U^2+2U\dot{x})\left(\frac{dC_D(\alpha)}{d\alpha}\sin\alpha + C_D(\alpha)\cos\alpha + \frac{dC_L(\alpha)}{d\alpha}\cos\alpha - C_L(\alpha)\sin\alpha\right)$$

letting $\alpha = 0$,

$$\frac{\partial F_z}{\partial \alpha}\Big|_{\alpha=0} = -0.5\rho B\,(U^2 + 2U\dot{x})\left(C_D + \frac{dC_L}{d\alpha}\right) \tag{2.28}$$

From Fig. 2.2 , for a small angle, $\alpha \doteq z / U$, the equation (2.27) becomes:

$$F_z = -0.5\rho B\,(U^2 + 2U\dot{x})\left(C_D + \frac{dC_L}{d\alpha}\right)\frac{\dot{z}}{U}$$

$$= -0.5\rho B\left(C_D + \frac{dC_L}{d\alpha}\right) U\dot{z} \tag{2.29}$$

The equation (2.29) expresses the vertical aerodynamic damping force due to the deck motion in vertical direction. Similarly, if the equation of motion in vertical direction is in the form:

$$m\,(\ddot{z} + 2\,\zeta_s\,\omega_z\,\dot{z} + \omega_z^2\,z) = F_z \tag{2.30}$$

where ω_z is circular frequency in vertical direction. By substituting (2.29) to (2.30), the vertical aerodynamic damping ratio can be obtained

$$\zeta_{az} = \frac{\rho UB}{4m\omega_z}\left(\frac{dC_L}{d\alpha} + C_D\right) \tag{2.31}$$

The equation (2.31) gives aerodynamic damping ratio in vertical oscillation direction.

As mentioned before, only horizontal and vertical responses of the bridge deck are treated in the present analysis. Based on the quasi-steady theory, the aerodynamic forces acting on the bridge deck are aerodynamic damping forces caused by deck motion and buffeting forces induced by the velocity fluctuations of the oncoming flow. In other words, the equations of motion of the bridge deck both in horizontal and vertical directions can be expressed as:

$$m\left(\ddot{x} + 2\zeta_x \omega_x \dot{x} + \omega_x^2 x\right) = F_{bx}(t) \tag{2.32}$$

$$m\left(\ddot{z} + 2\zeta_z \omega_z \dot{z} + \omega_z^2 z\right) = F_{bz}(t) \tag{2.33}$$

where ζ_x and ζ_z are total damping ratio in x and z directions which are written as

$$\zeta_x = \zeta_s + \zeta_{ax} \tag{2.34}$$

$$\zeta_z = \zeta_s + \zeta_{az} \tag{2.35}$$

ζ_{ax} and ζ_{az} are given in (2.26) and (2.31). $F_{bx}(t)$ and $F_{bz}(t)$ are buffeting forces for unit length caused by fluctuating components of velocities. From (2.10) and (2.11), they can be expressed as:

$$F_{bx}(t) = 0.5\rho U^2 B\left[C_D \frac{2u(t)}{U} + \frac{dC_D}{d\alpha}\frac{w(t)}{U}\right] \tag{2.36}$$

$$F_{bz}(t) = 0.5\rho U^2 B \left[C_L \frac{2u(t)}{U} + \left(\frac{dC_L}{d\alpha} + C_D \right) \frac{w(t)}{U} \right] \qquad (2.37)$$

2.2.2 Equations of Motion

In this section, the analysis procedure for a bridge response assumes that a preliminary vibrational analysis of a bridge structure has been made, yielding a series of natural vibration modes and corresponding frequencies.

Consider a line-like structure under aerodynamic forces which are aerodynamic damping forces and buffeting forces, as shown in Fig. 2.3. Let $q_i(t)$ be the corresponding time-dependent generalized coordinates, and $\Phi_{xi}(y)$ and $\Phi_{zi}(y)$ are horizontal and vertical mode shapes, respectively. The equations of motion in x and z directions can be expressed as

$$x(y, t) = \sum_i q_i(t)\, \Phi_{xi}(y) \qquad (2.38)$$

$$z(y, t) = \sum_i q_i(t)\, \Phi_{zi}(y) \qquad (2.39)$$

By introducing (2.38) and (2.39) to (2.32) and (2.33), the results are multiplied through by mode shapes and integrated over the bridge span l, yielding

$$\ddot{q}_i(t) + 2\zeta_{xi}\, \omega_{xi}\, \dot{q}_i(t) + \omega_{xi}^2\, q_i(t) = F_{xi}(t) / M_{xi} \qquad (2.40)$$

$$\ddot{q}_i(t) + 2\zeta_{zi}\,\omega_{zi}\,\dot{q}_i(t) + \omega_{zi}^2\,q_i(t) = F_{zi}(t) / M_{zi} \qquad (2.41)$$

where M_{xi} and M_{zi} are generalized mass in x and z directions, which are given by

$$M_{xi} = \int_0^l m(y)\,\Phi_{xi}^2(y)\,dy \qquad (2.42)$$

$$M_{zi} = \int_0^l m(y)\,\Phi_{zi}^2(y)\,dy \qquad (2.43)$$

The generalized buffeting forces $F_{xi}(t)$ and $F_{zi}(t)$ have the form

$$F_{xi}(t) = \int_0^l F_{bx}(t)\,\Phi_{xi}(y)\,dy \qquad (2.44)$$

$$F_{zi}(t) = \int_0^l F_{bz}(t)\,\Phi_{zi}(y)\,dy \qquad (2.45)$$

Generally the higher mode contribution to dynamic response can be negligible compared with the fundamental mode. In this thesis , only the first mode shape is used in the calculation of the buffeting response. If $\Phi_x(y)$ and $\Phi_z(y)$ express the first mode in x and z directions, respectively, the equations of the motion can be simply written as

$$\ddot{q}(t) + 2\,\zeta_x\,\omega_x\,\dot{q}(t) + \omega_x^2\,q(t) = \frac{1}{M_x}\int_0^l F_{bx}(t)\,\Phi_x(y)\,dy \qquad (2.46)$$

$$\ddot{q}(t)+2\zeta_z \omega_z \dot{q}(t)+\omega_z^2 q(t) = \frac{1}{M_z}\int_0^l F_{bz}(t)\,\Phi_z(y)\,dy \qquad (2.47)$$

Considering the equations (2.36) and (2.37) , the generalized forces corresponding to the first mode shape both in x and z directions can be expressed as:

$$F_x(t) = 0.5\rho B\int_0^l \left[\, 2C_D\, u(t) + \frac{dC_D}{d\alpha} w(t) \,\right] \Phi_x(y)\,dy \qquad (2.48)$$

$$F_z(t) = 0.5\rho B\int_0^l \left[\, 2C_L\, u(t) + \left(\frac{dC_L}{d\alpha} + C_D\right) w(t) \,\right] \Phi_z(y)\,dy \qquad (2.49)$$

2.2.3 Power Spectra of Generalized Forces and Velocity Fluctuations

The spectra of generalized forces can be obtained from (2.48) and (2.49), if the spectra of the fluctuating components u(t) and w(t) and their cross correlation spectrum are known. The expressions of the generalized force spectra are as follows:

$$S_{Fx}(f) = (0.5\rho UB)^2\int_0^l\int_0^l \left[4C_D^2\, S_{uu}(y,y',f) + \left(\frac{dC_D}{d\alpha}\right)^2 S_{ww}(y,y',f) + 4\,C_D\left(\frac{dC_D}{d\alpha}\right) S_{uw}(y,y',f)\,\right] \Phi_x(y)\,\Phi_x(y')\,dy\,dy' \qquad (2.50)$$

$$S_{Fz}(f) = (0.5\rho UB)^2 \int_0^l \int_0^l [\, 4C_L^2\, S_{uu}(y,y',f) + \left(\frac{dC_L}{d\alpha} + C_D\right)^2 S_{ww}(y,y',f)$$

$$+4C_L \left(\frac{dC_L}{d\alpha} + C_D\right) S_{uw}(y,y',f)\,] \Phi_z(y)\Phi_z(y')\, dy\, dy' \qquad (2.51)$$

Usually, the cross-correlation spectrum $S_{uw}(y,y', f)$ is negligible compared to the other terms, therefore, the equations (2.50) and (2.51) will simplify as:

$$S_{Fx}(f) = (0.5\rho UB)^2 \int_0^l \int_0^l [4C_D^2\, S_{uu}(y,y',f) + \left(\frac{dC_D}{d\alpha}\right)^2 S_{ww}(y,y',f)]\Phi_x(y)\Phi_x(y')dy\, dy' \qquad (2.52)$$

$$S_{Fz}(f) = (0.5\rho UB)^2 \int_0^l \int_0^l [4C_L^2\, S_{uu}(y,y',f) + \left(\frac{dC_L}{d\alpha} + C_D\right)^2 S_{ww}(y,y',f)]\Phi_z(y)\Phi_z(y')dydy' \qquad (2.53)$$

where $S_{uu}(y,y', f)$ and $S_{ww}(y,y', f)$ are the cross-spectral density functions. If along-span coherence is taken into account, the cross-spectra may be expressed in the form:

$$S_{uu}(y, y', f) = S_u(f)\, \tilde{R}_u(y, y', f) \qquad (2.54)$$

$$S_{ww}(y, y', f) = S_w(f)\, \tilde{R}_w(y, y', f) \qquad (2.55)$$

where $\tilde{R}_u(y,y',f)$ and $\tilde{R}_w(y,y',f)$ are called coherence functions or correlation coefficients,

a simple expression was given by Davenport [7] as follows:

$$\tilde{R}(y, y', f) = \exp\{-c \frac{f|y - y'|}{U}\} \tag{2.56}$$

where c is a coherence coefficient or a decay factor of correlation coefficient which is roughly 7 ~ 10.

In the equations (2.54) and (2.55), Su (f) and Sw (f) are defined as wind spectra for the u(t) and w(t) components of turbulence. There are a variety of spectral expressions available for modelling the velocity fluctuations. Based on these forms widely used in civil engineering, the expressions of von Karman (1948) and Kaimal's forms (1972) are used in the present analysis which are listed as follows :

(1) von Karman spectra

u-component of turbulence

$$Su(f) = \frac{4\sigma u^2 \overset{x}{L}u}{U} [1 + 70.8 (\frac{f \overset{x}{L}u}{U})^2]^{-5/6} \tag{2.57}$$

w-component of turbulence

$$Sw(f) = \frac{2\sigma w^2 \overset{z}{L}w [1+188.8 (f \overset{z}{L}w / U)^2]}{U [1+ 70.78 (f \overset{z}{L}w / U)^2]^{11/6}} \tag{2.58}$$

where σu and σw are the root-mean-square values of fluctuating velocity component u and

w, which are given in terms of turbulence intensities Iu and Iw

$$Iu = \sigma u / U \tag{2.59}$$

$$Iw = \sigma w / U \tag{2.60}$$

L_u^x and L_w^z are the integral scales of turbulence. These expressions are based on the assumption that the flow field is characterized by homogeneous, isotropic turbulence.

(2) Kaimal spectral forms are based on an extensive field study called the Kansas experiments and take the following expressions:

u-component of turbulence

$$Su(f) = \frac{\sigma u^2}{f} \frac{22\,n}{(1 + 33\,n)^{5/3}} \tag{2.61}$$

w-component of turbulence

$$Sw(f) = \frac{\sigma w^2}{f} \frac{1.3\,n}{1 + 5.3\,n^{5/3}} \tag{2.62}$$

in which $n = f Z / U$, Z is the height above ground.

2.2.4 Response Power Spectra

Once the intensities and scales of turbulence are given or measured by experiment,

the cross-spectral expressions can be determined by (2.54) and (2.55). The response spectra can be obtained as follows:

$$S_{qx}(f) = \frac{1}{\omega_x^4 M_x^2} |H_x(f)|^2 S_{Fx}(f) \tag{2.63}$$

$$S_{qz}(f) = \frac{1}{\omega_z^4 M_z^2} |H_z(f)|^2 S_{Fz}(f) \tag{2.64}$$

where $|H_x(f)|^2$ and $|H_z(f)|^2$ are called the mechanical admittance which are expressed as

$$|H_x(f)|^2 = \frac{1}{[1-(f/f_x)^2]^2 + [2\zeta_x (f/f_x)]^2} \tag{2.65}$$

$$|H_z(f)|^2 = \frac{1}{[1-(f/f_z)^2]^2 + [2\zeta_z (f/f_z)]^2} \tag{2.66}$$

in which f_x and f_z are the first natural frequency corresponding horizontal and vertical vibration; ζ_x and ζ_z are total damping ratios given in (2.34) and (2.35).

The variance of the response can be obtained by integrating (2.63) and (2.64)

$$\sigma_{qx}^2 = \int_0^\infty S_{qx}(f)\, df = \frac{1}{\omega_x^4 M_x^2} \int_0^\infty |H_x(f)|^2 S_{Fx}(f)\, df \tag{2.67}$$

$$\sigma_{qx}^2 = \int_0^\infty S_{qz}(f)\,df = \frac{1}{\omega_z^4 M_z^2} \int_0^\infty |H_z(f)|^2 S_{Fz}(f)\,df \qquad (2.68)$$

2.3 Effects of Yaw Angles on Bridge Response

Conventional buffeting analytical procedures are only applicable for winds normal to the bridge span. However, a strong wind does not always have the highest probability of occurrence from the direction normal to the bridge span. It is possible to have significant fatigue damage to a bridge from winds with horizontally skewed angles (yawed wind). An example is a long-span cable-stayed bridge during its erection stage. Particularly, the most critical situation is just before the main span of the cable-stayed bridge is closed, during which the bridge has much less stiffness than a completed bridge. The turbulent wind can shake the two long cantilever structures supported by cables. Some experimental investigations have also focussed on winds with horizontal skew angles, particularly in cases of cable-stayed bridges during their erection stages. These experimental results show a higher response to yawed wind.

Recently some analytical approaches have also been used to predict the buffeting response when the horizontal yaw angles are considered. Xie et al [53] presented a buffeting analysis of long span bridge under yawed wind. The analysis was carried out by introducing the concept of effective values of mean wind speed, deck width and scales of turbulence. But this approach was limited to small yaw angle cases. It can not be applied to bridges with unsupported free ends corresponding to cable-stayed bridges during their erection.

Kimura [24] developed a modified buffeting analysis to explain his experimental results by introducing the concept of effective wind speed as either chordwise or lengthwise components of the flow velocity, called the cosine or sine case. Meanwhile, a correction factor for the lift-curve slope due to the effect of the small aspect ratio is considered based on the measured results by Winter [52]. The approach can be applied to predict the buffeting response of the models with a flat plate cross-section under yawed wind by separately considering normal and parallel wind components. The calculated results showed a tendency similar to his experimental data. The application of the modified buffeting analysis was still limited to idealized models with flat plate sections and the calculations were restricted to vertical bending oscillation as well.

Scanlan attempted a similar modified buffeting analysis and also considered the effect of the aspect ratio on lift characteristics based on Eiffel's test results [34]. However, the analytical results have little support from experiments.

Two full cable-stayed bridge models, the Normandy Bridge and the Kao Ping Hsi Bridge, were tested at the Martin Jensen Wind Tunnel of the Danish Maritime Institute [5, 25]. The former, with a centre-span of 856 m, is the longest clear span cable-stayed bridge in the world. The latter is a single-tower cable-stayed bridge. The wind tunnel tests of these bridges during their construction stages were conducted. Experimental data show that the maximum dynamic response in lateral bending was reached with 35° yaw angle wind for the Normandy Bridge. The maximum value of fluctuating cable tension was found at the yaw angle of 20° to 30° for the same bridge. For the Kao Ping Hsi Bridge, in construction stage, the dynamic cable force is approximately three times larger than in service condition .

It is obvious that the consideration of the yaw angle effects on cable-stayed bridges is very important because it may significantly change the prediction of dynamic response.

2.4 Modified Buffeting Analysis

In this section, the modified buffeting analysis for predicting vertical bending is first explained by following the approach proposed by Kimura [24]. It is then extended by the present author for the prediction of lateral buffeting response.

The procedure of the modified buffeting analysis is similar to the conventional buffeting theory. However, in the modified buffeting approach , the effects of yawed wind action are considered by introducing the concept of effective wind speed. To obtain the generalized aerodynamic forces acting on a bridge deck, the strip theory can be used as an approximation, where the generalized forces are obtained by integrating the two dimensional aerodynamic forces acting on each narrow strip sliced along the wind direction. As stated previously, the aerodynamic forces are the aerodynamic damping force and buffeting force based on the quasi-steady approximation.

2.4.1 Effective Wind Speed

The concept of effective wind speed is based on the fact that if an infinitely long plate is placed in the flow with no viscosity , the distribution of the aerodynamic forces along the span-wise of the plate is the same whenever the plate is moving along its longitudinal direction. As also explained by Fig. 2.4, the aerodynamic forces acting on an infinite plate depend only on the velocity component normal to the longitudinal axis of the plate and the velocity component V (if the plate is moving with velocity V) does not have any effect. If the relative wind velocity Ur is considered, Ur $\cos\beta$ can be defined as the effective wind velocity which actually generates the aerodynamic effects on the structure. Fig. 2.4 is an example with an infinitely long plate under yawed wind.

Although long span bridges are not infinitely long, the basic concept as described above can be as an approximation in the present analysis, i.e. effective wind speed is taken as the velocity component normal to the leading edge of bridges. For cable-stayed bridges

under construction, or cantilever structures, they have two leading edges, one is the along-span side and the other is the end of the bridge or the free end of the structure as shown in Fig. 2.5. The corresponding effective wind speeds become $Uc = U \cos\beta$ and $Us = U \sin\beta$ respectively.

When Uc is considered as the effective wind speed, it is called the cosine case, and similarly, the sine case means when effective wind speed Us is considered. By introducing the cosine and sine cases, the buffeting analysis can be developed for both cases with yaw angles as given in the following section.

2.4.2 Generalized Aerodynamic Forces

The aerodynamic forces acting on a bridge deck are buffeting forces based on the quasi-steady theory. To calculate the generalized aerodynamic forces, the so-called strip theory is applied to the modified buffeting analysis. As with the usual strip theory approximation, aerodynamic forces acting on each strip parallel to the mean wind direction are first calculated, and total aerodynamic forces are then obtained by integrating the forces acting on each strip. However, it should be noted that the aerodynamic coefficients are different for each case in which effective wind speed is normal or parallel to the longitudinal axis of the bridge. In other words, the lengthwise component and chordwise component of the cosine and sine cases are simply a reverse of each other.

First, the buffeting analysis for the prediction of the vertical bending for the cosine and sine cases is presented. With the strip theory and quasi-steady approximation, the lift forces caused by fluctuating velocity w-component corresponding to the cosine and sine cases can be expressed as

$$dL_c(y,t) = 0.5\rho U_c^2 (dS) C_{L\alpha} \frac{w(y,t)}{U_c}$$

$$= 0.5\rho U \cos\beta \, C_{L\alpha} \, w(y,t) \, dS \qquad (2.69)$$

$$dL_s(x,t) = 0.5\rho U \sin\beta\,(dS)\,\tilde{C}_{L\alpha}\, w(x,t) \tag{2.70}$$

where dL_c and dL_s are the lift forces on the strip; $C_{L\alpha} = dC_L / d\alpha$ and $\tilde{C}_{L\alpha} = d\tilde{C}_L / d\alpha$, which are the lift slopes of the model under the wind with $\beta = 0°$ and $\beta = 90°$, respectively; dS is the area of a strip.

It can be seen that the deflection inside a strip is the same in the cosine case, and in the sine case it is the same as the mode shape of the bridge model. The generalized buffeting forces on the strip corresponding to the cosine and sine cases would be

$$\begin{aligned} dL_{cg} &= dL_c\,\Phi_z(y) \\ &= 0.5\rho U\cos\beta\, C_{L\alpha}\, w(y,t)\,\Phi_z(y)\,dS \end{aligned} \tag{2.71}$$

$$dL_{sg} = 0.5\rho U(db)\sin\beta\, w(x,t)\int_0^{ls} \tilde{C}_{L\alpha}(s)\Phi_z(s)\,ds \tag{2.72}$$

in which db is the width of the strip ; ls is the length of the strip; $\Phi_z(s)$ is the mode shape along the strip; $C_{L\alpha}(s)$ expresses the lift force distribution along the strip and s is the coordinate along the strip with the origin at the end edge. The distribution of $C_{L\alpha}(s)$ for thin flat plates is taken from McCormick [27] as shown in Fig. 2.6. The area between $C_{L\alpha}(s)$ and the horizontal axis is equal to $\tilde{C}_{L\alpha}$. It is used in the following calculation as an approximation.

The overall generalized aerodynamic forces are obtained by integrating (2.71) and (2.72) along the strip. Because the resultant lift force on the strip is acting at the quarter point chordwise from the leading edge for the cosine case, the generalized forces per unit span over the bridge model can be expressed as

$$L_{cg} = 0.5\rho UB\cos\beta\, C_{L\alpha}\int_{e}^{l+e} w(y,t)\Phi_z(y)\,dy \tag{2.73}$$

$$L_{sg} = 0.5\rho U\sin\beta\,(\int_{0}^{ls}\tilde{C}_{L\alpha}(s)\,\Phi_z(s)\,ds)\int_{0}^{B} w(x,t)\,dx \tag{2.74}$$

where $e = B\,tg\,\beta/4$, and $\Phi_z(y) = \Phi_z(l)$, when $y > l$.

It should be explained that the equations (2.73) and (2.74) correspond to the case of a flat plate model, in which $C_L = 0$, and C_D is negligible. Generally, the generalized buffeting forces caused by u and w components of fluctuating velocities can be written in the following forms in terms of the equation (2.10):

$$L_{cg} = 0.5\rho UB\cos\beta\int_{e}^{l+e}[\,2C_L\,u(y,t)+(C_{L\alpha}+C_D)\,w(y,t)\,]\Phi_z(y)dy \tag{2.75}$$

$$L_{sg} = 0.5\rho U\sin\beta\{\int_{0}^{ls}2\tilde{C}_L\Phi_z(s)ds\int_{0}^{B}u(x,t)dx$$

$$+\int_{0}^{ls}(\tilde{C}_{L\alpha}(s)+\tilde{C}_D)\,\Phi_z(s)ds\int_{0}^{B}w(x,t)\,dx\,\} \tag{2.76}$$

where $\tilde{C}_L$ and $\tilde{C}_D$ are lift and drag coefficients corresponding to the sine case.

Using the same concept of the effective wind speed, lateral buffeting forces acting on a strip can be obtained, which are caused by the aerodynamic drag force. Considering

a cantilever deck ,as shown in Fig. 2.7, the effective wind speeds corresponding to the cosine and the sine cases are:

$$U_c = (U + u)\cos\beta - v\sin\beta \tag{2.77}$$

$$U_s = (U + u)\sin\beta + v\cos\beta \tag{2.78}$$

According to the strip theory and the quasi-steady approximation, the drag force acting on a strip along the effective wind speed direction can be expressed as

$$dD_c(y,t) = 0.5\,\rho U_c^2\, C_D\, dS \tag{2.79}$$

$$dD_s(x,t) = 0.5\rho\, U_s^2\, \tilde{C}_D\, dS \tag{2.80}$$

substituting (2.77) and (2.78) to above expressions, and the terms involving the products of u and v can be neglected, the drag forces caused by the mean wind speed U and u, v components of fluctuations become:

$$dD_c(y,t) = \rho U C_D\,(dS)[u(y,t)\cos^2\beta - v(y,t)\cos\beta\sin\beta] \tag{2.81}$$

$$dD_s(x,t) = \rho U\, \tilde{C}_D\,(dS)[u(x,t)\sin^2\beta - v(x,t)\cos\beta\sin\beta] \tag{2.82}$$

where C_D and $\tilde{C}_D$ are the drag force coefficients of the model with $\beta = 0°$ and $\beta = 90°$.

The generalized drag forces acting on a strip corresponding to the cosine and sine cases will be:

$$dD_{cg}(y,t) = dD_c(y,t)\,\Phi_x(y)$$

$$= \rho U C_D [\, u(y,t)\cos^2\beta - v(y,t)\cos\beta\sin\beta](dS)\,\Phi_x(y) \qquad (2.83)$$

$$dD_{sg}(x,t) = \rho U \tilde{C}_D(db)[\int_0^{ls}\Phi_x(s)ds]\,[u(x,t)\cos^2\beta - v(y,t)\cos\beta\sin\beta] \qquad (2.84)$$

The overall generalized aerodynamic forces can be obtained by integrating (2.83) and (2.84) , they can be expressed as:

$$D_{cg}(y,t) = \rho U C_D B\int_0^{l}[u(y,t)\cos^2\beta - v(y,t)\cos\beta\sin\beta\,]\Phi_x(y)dy \qquad (2.85)$$

$$D_{sg}(x,t) = \rho U \tilde{C}_D(\int_0^{ls}\Phi_x(s)ds\,)\int_0^{B}[u\cos^2\beta - v\cos\beta\sin\beta\,]dx \qquad (2.86)$$

The generalized aerodynamic forces both of lateral and vertical directions acting on a bridge deck can be determined by the equations (2.75), (2.76), (2.85) and (2.86) as long as the aerodynamic force coefficients are known.

2.4.3 Response Power Spectra

As with the conventional buffeting analysis, the spectral density of the generalized aerodynamic forces can be expressed as follows:

(1) Vertical response caused by the lift forces:

(a) Cosine case

$$S_{Lc}(f) = (\rho U B C_L \cos\beta)^2 \int_{c}^{l+c}\int_{c}^{l+c} S_{uu}(y,y',f)\,\Phi_z(y)\Phi_z(y')\,dydy'$$

$$+[\,0.5\rho U B(C_{L\alpha}+C_D)\cos\beta]^2 \int_{c}^{l+c}\int_{c}^{l+c} S_{ww}(y,y',f)\Phi_z(y)\Phi_z(y')dydy' \qquad (2.87)$$

(b) Sine case

$$S_{Ls}(f) = (\rho U \tilde{C}_L \sin\beta \int_0^{ls} \Phi_z(s)ds\,)^2 \int_0^B\int_0^B S_{uu}(x,x',f)dxdx'$$

$$+ [\,0.5\rho U \sin\beta \int_0^{ls} (\,\tilde{C}_{L\alpha}(s) + \tilde{C}_D\,)\Phi_z(s)\,ds\,]^2 \int_0^B\int_0^B S_{ww}(x,x'f)\,dxdx' \qquad (2.88)$$

(2) Horizontal response caused by the drag forces:

(a) Cosine case

$$S_{Dc}(f) = (\rho U C_D B\cos^2\beta)^2 \int_0^l\int_0^l S_{uu}(y,y'f)\,\Phi_x(y)\Phi_x(y')\,dydy'$$

$$+ (\rho U C_D B\cos\beta\sin\beta\,)^2 \int_0^l\int_0^l S_{vv}(y,y',f)\,\Phi_x(y)\Phi_x(y')\,dydy' \qquad (2.89)$$

(b) Sine case

$$S_{Ds}(f) = (\rho U \tilde{C}_D \cos^2\beta \int_0^l \Phi_x(s)ds\,)^2 \int_0^B\int_0^B S_{uu}(x,x',f)\,dxdx'$$

$$+ (\rho U \tilde{C}_D \cos\beta\sin\beta \int_0^l \Phi_x(s)ds\,)^2 \int_0^B\int_0^B S_{vv}(x,x',f)\,dxdx' \qquad (2.90)$$

Generally , the aerodynamic admittance should be considered in the buffeting analysis due to the effect of the non-uniform flow field on aerodynamic force characteristics. In the present analysis, the aerodynamic admittance is assumed to be unity as an approximation, since its magnitude can not be identified.

By using above expressions, the response power spectra can be obtained in both horizontal and vertical directions as

$$S_{qx}(f) = \frac{S_D(f)}{\omega_x^4 \, M_x^2} \, |H_x(f)|^2 \tag{2.91}$$

$$S_{qz}(f) = \frac{S_L(f)}{\omega_z^4 \, M_z^2} \, |H_z(f)|^2 \tag{2.92}$$

where $S_D(f)$ is $S_{Dc}(f)$ or $S_{Ds}(f)$, and $S_L(f)$ is $S_{Lc}(f)$ or $S_{Ls}(f)$ for the cosine or sine cases, respectively; ω_x and ω_z are natural circular frequencies of the first mode in lateral and vertical bending vibration; M_x and M_z are generalized mass given by (2.42) and (2.43), corresponding to the first mode shape; $|H_x(f)|^2$ and $|H_z(f)|^2$ are mechanical admittances given by (2.65) and (2.66).

The variance of the response corresponding to the generalized coordinate q is then obtained by

$$\sigma_{qx}^2 = \int_0^\infty S_{qx}(f) \, df \tag{2.93}$$

$$\sigma_{qz}^{\,2} = \int_0^{\infty} S_{qz}(f)\, df \qquad (2.94)$$

2.4.4 Evaluation of Aerodynamic Parameters

It is obvious that buffeting response of a bridge structure depends not only on the structural properties, but also on the characteristics of turbulent wind . For a cable-stayed bridge, all parameters used in the calculation of the horizontal and vertical response can be summarized as follows:

(1) Structural parameters:
- . Geometrical dimension
- . Mass and stiffness distribution of a bridge
- . Natural frequencies and corresponding mode shapes
- . Structural damping

(2) Aerodynamic parameters:
- . Turbulence intensities
- . Integral scales of turbulence
- . Velocity spectra

(3) Interaction parameters:
- . Drag and lift force coefficients
- . Aerodynamic damping
- . Aerodynamic force correlation
- . Aerodynamic admittance

In the present analysis and calculation of the buffeting response, the structural parameters are obtained from the experiments. However, some aerodynamic parameters and interaction factors used in the modified buffeting analysis have to be evaluated by considering the effective wind speed, for both cosine and sine cases.

It has been established that the aerodynamic lift coefficient and its slope for a flat plate can be identified as a function of a structural aspect ratio AR. For a bridge, aspect ratio is defined as a ratio of its span length to width. For cosine and sine cases, the aspect ratio is defined as $(AR)_c = l / B$ and $(AR)_s = B / l$, respectively.

For small aspect ratio of the sine case, ($AR \leq 1/3$, say), additional considerations are needed to estimate the lift slope. Bisplinghoff [1] suggested the linear theory for a delta wing having a small aspect ratio

$$\tilde{C}_{L\alpha} = \frac{\pi}{2} AR \tag{2.95}$$

in which the aspect ratio AR was defined as l^2 / S where l is the length of the delta wing, and S is the wing area. The expression is used in the calculation for sine case with linear theory. In fact, for a flat plate with the small aspect ratio, the effect of some additional lift caused by the vortices formed along the sides of the flat plate is evident and should be considered. This effect causes nonlinear changes of the lift force coefficient C_L with the angle of attack. An example is shown in Fig. 2.8 (Gersten , 1960), which is the lift force coefficient C_L vs. the angle of attack α for a rectangular plate with $AR = 0.2$.

It can be seen that the lift slope based on the linear theory at $\alpha = 0°$ obviously gives a lower estimate. In order to consider the nonlinear effect for the small aspect ratio, the equivalent lift slopes are evaluated based on the measured results. If measured lift coefficients which change nonlinearly with angle of attack are known, the average lift slope between zero and peak angle of attack α' is expressed as $Cl_{:\,meas}(\alpha') / \alpha'$, where $Cl_{:\,meas}$

is the measured lift coefficient.

In the following calculation, as an approximation, the equivalent lift slope considering the nonlinear effect was taken and interpolated from the measured results of Winter [52], as shown in Fig. 2.9, which is the normal force coefficient C_n against the angle of attack for various aspect ratios.

To explain how to apply the measured results, the relationship of the lift, drag and normal forces is shown in Fig. 2.10, the normal force F_n may be expressed by

$$F_n = 0.5\,\rho U^2 A\, C_n \tag{2.96}$$

where A is the plate area; and C_n is called the normal force coefficient. The lift and drag forces are related to F_n by

$$L = F_n \cos\alpha \tag{2.97}$$

$$D = F_n \sin\alpha \tag{2.98}$$

in which the lift slope becomes

$$\tilde{C}_{L\alpha} = \frac{dC_n}{d\alpha} \cos\alpha - C_n \sin\alpha \tag{2.99}$$

where the angle of attack is the peak angle of attack α' which is taken as w'/U, where w' is a possible maximum of w calculated by assuming Gaussian distribution of w (i.e. $w' = 3.6\,\sigma_w$). The equation (2.99) gives the lift slope for small aspect ratio .

In the following analysis, for sine case, the buffeting response for vertical motion will be referred to as linear and nonlinear results, depending on the lift slope given in (2.95)

and (2.99), the former is referred to as linear and the latter is referred to as nonlinear.

Another important parameter is the aerodynamic damping ratio ζ_a as stated before. In the buffeting analysis, it is often a large part of the total damping effects. Based on the conventional buffeting analysis, the aerodynamic damping ratio given by (2.26) and (2.31) is only the case of wind normal to the bridge span. However, there has not been an established theoretical means to evaluate the aerodynamic damping ratio under yawed wind. In the present analysis, it is assumed to be proportional to cos β, which can be expressed as :

$$\zeta_a = \zeta_{ao} \cos \beta \tag{2.100}$$

where ζ_{ao} is ζ_{ax} or ζ_{az} given by (2.26) and (2.31). The same assumption was used by Kimura [24] for the analysis of flat plate models.

Once all structural and aerodynamic parameters of the bridge are determined, the root-mean-square (rms) response of the bridge can be predicted.

Chapter 3
Comparison of Analytical and Experimental Results

3.1 Introduction

Wind tunnel studies have clearly indicated that buffeting response is particularly important for long-span cable-stayed bridges during their construction under yawed wind conditions [5,25]. In order to compare the theoretical analysis with experimental observations, a modified buffeting approach has been developed to calculate buffeting response both in lateral and vertical bending oscillations under yawed wind.

Kimura [24] developed a modified buffeting approach to include wind yaw angle effects in buffeting calculation and compared the analytical results with wind tunnel test results of flat plate models. After a computer program was developed for the present study, it was also applied to these flat plate models to confirm its validity. The computer program was then applied to two aeroelastic models of cable-stayed bridges, i.e. the Normandy Bridge and the Kao Ping Hsi Bridge. The wind tunnel tests of the both bridge models were carried out at the Martin Jensen Wind Tunnel of the Danish Maritime Institute, Denmark in 1993 and the author was given access to their experimental results. The wind tunnel investigations examined the critical stages of the bridges during their erection for different wind directions.

Calculated results are shown together with the corresponding experimental results in this chapter. The calculated root-mean-square responses of both cosine and sine cases are shown in each figure, and for the sine case, the results for both " linear " and " nonlinear " are included in the vertical bending response. As discussed previously, the effective wind comes from a direction normal to the long axis of the model in cosine cases, and it comes from the free end of the model in sine case.

Usually, the higher mode contribution to the response is negligible compared with the

fundamental mode. For this reason, only first mode corresponding to both lateral and vertical bending oscillations is used in the following calculation.

3.2 Buffeting Response of Cantilever Models

The wind tunnel tests of a series of cantilever flat plate models were carried out by Kimura [24], of which only vertical deflection was allowed. Three typical models with different width were chosen for the calculation of buffeting response to be compared with the experimental results.

The model characteristics, the flow conditions and the lift slope used in the present analysis are listed in Tables 3.1 and 3.2. The velocity spectrum for w-component of turbulence is approximated by the spectrum defined by Kaimal et al (1972), i.e. spectral equation given in (2.62).

Table 3.1 Model characteristics and flow conditions

Model No.	Width B(mm)	Length l (mm)	Thickness (mm)	Freq. (HZ)	Damping ratio (%)	Tur. int. (%)	Scale length(mm)
1	25.4				0.45	Iu=8	Lu =24
2	50.8	305	0.8	7.1	0.54	Iw=6.2	Lw =10
3	102				0.58		

Table 3.2 Lift slope used in the calculation

Model No.	Cosine case	Sine case	
		Linear	Nonlinear
1	5.0	0.13	0.68
2	4.2	0.26	0.96
3	3.1	0.52	1.20

Figs. 3.1 through 3.3 show comparison of the calculated results against wind yaw angles for models with different width when wind speed is 3 m/s. The ordinate is the vertical deflection at the model tip and is made dimensionless by dividing by the model width.

The comparison of the calculated results with the experimental results shows that

(1) For the response of $\beta = 0°$ where wind comes normal to the model span, the calculated results generally compare well with the experimental results.

(2) For the response of $\beta = 90°$ where wind comes from the free end direction, the experimental data are between so-called " linear" and " nonlinear " results.

(3) The variation of the model response vs. wind angles generally agrees for yaw angle $|\beta| < 50°$ by cosine case; For $50° < |\beta| < 80°$, in which cosine and sine cases intersect, the experimental data show smooth transition. The calculated results could not show the same tendency due to the choice of the method including both cosine and sine cases.

Further discussions are given in the next chapter.

3.3 Buffeting Response of the Normandy Bridge

The superstructure of the Normandy Bridge has a main span of 856 m. The main span is composed of two parts, a 116 m concrete box girder, extending from each tower, followed by a 624 m steel-box girder for the central portion of the span. Figs. 3.4 and 3.5 show prototype dimensions and the cross-section of the bridge. There are two towers of 202.7 m height on which the cables are anchored to support the bridge deck. A total of 92 stay cables are arranged in two vertical planes. The mean bridge deck elevation is 65 m above water.

The wind tunnel test of the Normandy bridge was conducted by the Danish Maritime Institute in 1993. An aeroelastic model of this bridge during its construction was built with a geometric scale of 1 : 150 shown in Fig. 3.6. The bridge model was tested for the most critical stage of this bridge during its erection; i.e., when a cantilever of 428 m is extended from a pylon with supporting cables. The wind tunnel testing investigated the buffeting response of this bridge, including both in lateral and vertical bending oscillations under full scale wind speeds from 10 m/s to 55 m/s at the bridge level.

The measured mode shapes corresponding to the first lateral and vertical modes are given in Figs. 3.7 and 3.8. The geometric dimension and mass distribution of the bridge model are shown in Fig. 3.9. The model characteristics are listed in Table 3.3. The turbulence of two different boundary layer flows are defined as exposure 1 and 2 as specified in Table 3.4. The aerodynamic force coefficients are given in Table 3.5. Velocity spectra were measured at the bridge deck level and were found to be similar to the so-called von Karman spectra given by (2.57) and (2.58).

Table 3.3 The model characteristics of the Normandy Bridge

Mode	Prototype freq. (HZ)	Model freq. (HZ)	Structural damping ratio (%)
Lateral	0.114	1.365	0.2
Vertical	0.214	2.350	0.4

Table 3.4 Wind conditions at the bridge site

Exposure	Turbulence intensities (%)	Length scales (m)	Decay factor Long.	Vert.
1	Iu = 9, Iw = 5	Lu = 200, Lw = 35	10	8
2	Iu = 13, Iw = 7	Lu = 100, Lw = 29	11	9

Table 3.5 Lift and drag coefficients and lift slope

Lift coefficient	Lift slope			Drag coefficient	
	Cosine	Sine (l)	Sine (n)	Cosine	Sine
-0.32	4.1	0.08	0.70	0.67	0.04

As described before, the aerodynamic force coefficients are different for cosine and sine cases. Table 3.5 shows these aerodynamic force coefficients corresponding to cosine and sine cases. For cosine case, the lift, drag and lift slope are taken from the section model testing results of the Normandy Bridge. For sine case, the equivalent lift slopes are referred to as linear and nonlinear results as stated in section 2.4.4, the former is given by (2.95); the latter is approximately obtained from the experimental results by Winter [52], including the drag coefficient of the sine case.

The buffeting calculation was attempted for both lateral and vertical response using the modified buffeting approach. The comparison of calculated and experimental results is shown in Figs. 3.10. through 3.21.

Figs. 3.10 and 3.11 show root-mean-square responses of both lateral and vertical deflection at the tip vs. wind speeds at bridge level, i.e. in the case of wind normal to the bridge span. Both analytical and experimental results show that dynamic response is proportional to wind speed.

Figs. 3.12 through 3.19 show buffeting response of both lateral and vertical deflection at the main span free end against yaw angles, corresponding to the full-scale wind speeds of 30 m/s, 33 m/s, 39 m/s and 44 m/s at the bridge level. There is general agreement between calculated and experimental results.

Fig. 3.18 also shows the effect of aerodynamic damping on buffeting response of this bridge. Different damping is used to calculate of lateral bending response, one is based on the equation (2.26) in terms of the quasi-steady assumption as the curve 2 in Fig. 3.18, another is obtained from measured total damping when wind is normal to the bridge span as the curve 1 in Fig. 3.18. It can been seen that the aerodynamic damping plays an important role in prediction of buffeting response of cable-stayed bridges.

Both velocity spectral expressions, von Karman's and Kaimal's forms , were used in the calculation shown in Figs. 3.20 and 3.21. It is found that there is no significant difference.

3.4 Buffeting Response of the Kao Ping Hsi Bridge

The Kao Ping Hsi Bridge (Taiwan) is an asymmetric one-tower cable-stayed bridge with a main steel span of 331 m and a concrete side span of 183 m, the width of the bridge girder is 34.5 m . The mean bridge deck elevation is 50 m . Figs. 3.22 and 3.23. show the general configuration of the Kao Ping Hsi Bridge and its cross section. Because of its asymmetric configuration, the bridge will have a very long cable-supported cantilever during its erection stage.

The wind tunnel investigation at the Martin Jensen Wind Tunnel of the Danish Maritime Institute included section model tests and 1:150 scale model tests with the configuration of the last construction stage and the in-service condition of the bridge. The full bridge model of the Kao Ping Hsi is shown in Fig. 3.24.

The test report [5] indicated that the maximum bridge deck buffeting response during construction is much larger than the response with its completed condition, as expected, due to less stiffness at this stage.

The model characteristics are given in Table 3.6. The aerodynamic force coefficients are listed in Table 3.7. The longitudinal and vertical turbulence intensities for the construction stage are 10% and 8%. The velocity spectra are compared to the Kaimal spectra.

Table 3.6 The model characteristics of the Kao Ping Hsi Bridge

Mode	Model freq. (HZ)	Structural damping ratio (%)	Mass distribution (Kg/m)
Lateral	1.88	0.20	0.894
Vertical	2.32	0.30	

Table 3.7 The aerodynamic force coefficients

Lift coefficient	Lift slope			Drag coefficients	
	Cosine	Sine (l)	Sine (n)	Cosine	Sine
-0.38	6.0	0.16	0.73	0.45	0.08

The buffeting response under yaw winds was measured at 5 different wind speeds, corresponding to full-scale wind speeds of approximately 20 m/s, 35 m/s, 50 m/s, 65 m/s and 80 m/s at the bridge deck level. The bridge response included vertical, lateral and torsional motion of the deck.

The buffeting response was calculated for both lateral and vertical bending oscillations during the bridge erection and was compared to the experimental results. Figs. 3.25 through

3.30 show the root-mean-square response of lateral and vertical deflection of main span free end against yaw angles.

The comparison of the calculated results with the experimental results shows that

(1) When wind comes normal to the bridge model span, the calculated results are about 1.5 - 2.0 times larger than the experimental results for both lateral and vertical displacements.

(2) The experimental results show that the vertical response of the bridge end is nearly constant for all yaw angles when wind speeds are 50 m/s, 64 m/s and 80 m/s at bridge deck level, but the lateral response shows irregularity with the yaw angles. The analytical results in vertical motion show the same tendency when yaw angles are between 0° and 70° , but calculated values are nearly 1.5 times larger than the measured data.

Chapter 4
Discussion

The buffeting response of cable-stayed bridges during their erection has been discussed in this thesis. The modified buffeting approach is further developed to predict lateral bending oscillation and the approach is applied to predict buffeting response of cable-stayed bridge models under yawed wind. The analytical results both in vertical and lateral bending oscillations are compared with the experimental results of cable-stayed bridge models, they are in general agreement. On the other hand, it is also been found that aerodynamic parameters play an important role in prediction of buffeting response of cable-stayed bridges.

The discussion in this chapter is based on a comparison of the analytical and experimental results given in Chapter 3. Discussed are some parameters in the prediction of the buffeting response of cable-stayed bridges during their construction stage.

4.1 Effect of Aerodynamic Damping

In the present buffeting analysis, the aerodynamic damping force is based on the quasi-steady assumption. The buffeting force is caused by the fluctuation of the oncoming flow, whereas the aerodynamic damping is caused by the movement of the structure itself. In the buffeting analysis procedure, it is important to include the aerodynamic damping together with the mechanical damping as explained in section 2.2.1, since it is often a fraction of the total damping effects.

Aerodynamic damping is a dominant factor in prediction of the buffeting response. However, there has not been an established theoretical means to evaluate the aerodynamic damping under yawed wind. In the present analysis, the aerodynamic damping under yawed

wind is assumed to be proportional to $\cos\beta$. The same assumption was used by Kimura [24] for the buffeting analysis of flat plate models.

It should be noted that for the vertical bending oscillation of flat plates, aerodynamic damping ratio is proportional to $\cos\beta$. This expression may not be applicable for bridges with box sections, such as the Normandy Bridge or the Kao Ping Hsi Bridge. On the other hand, even though wind is normal to the bridge span, the measured and analytical results are not in agreement. Fig. 4.1 shows the difference between the quasi-steady aerodynamic damping ratio and the experimental results for lateral motion of the Normandy Bridge. The measured data are significantly larger than the quasi-steady results.

By the comparison of the analytical and experimental results, when β is close to 0° (i.e. cosine case), the calculated results generally compare well with the experimental data if the measured aerodynamic damping is used in the calculation. For example, the vertical bending for the flat plate models as shown in Figs. 3.1 through 3.3 and the lateral deflection for the Normandy Bridge as shown in Fig.3.10 under wind normal to the bridge span.

For the vertical deflection response of both the Normandy Bridge and Kao Ping Hsi Bridge, the calculated results are greater than the experimental data. One reason is probably the evaluation of the aerodynamic damping which remains uncertain.

4.2 Effect of Turbulence Characteristics

The effect of turbulence can be discussed in terms of the turbulence intensity, the integral scales of turbulence or the velocity spectral density. These factors directly influence the results of the buffeting response prediction.

It can be easily shown that buffeting response is simply proportional to the turbulence intensity if other parameters are not influenced by turbulence intensity. The turbulence characteristics in wind tunnel test sections are not necessarily homogeneous. Because of the limited size of the flow field, both the turbulence scale and intensity would be different in the mean flow direction. The variation of the flow characteristics could influence the buffeting response of a bridge. In particular, when yaw angle $|\beta|$ is close to 90° (i.e. sine case), the bridge span is almost parallel to the flow direction and thus the flow characteristics may vary most significantly along the bridge span. In the present calculations, the possible variation of the flow characteristics along a bridge span was not considered. It can be concluded that the lateral bending response prediction using the flow characteristics at a model free end location would be larger than that using the flow characteristics at the model support location. The larger a bridge model dimension is, the more significant the effect on lateral bending response would be.

Another factor influencing buffeting response could be the general shape of velocity spectra. The von Karman's expressions of velocity spectrum were used in the calculation for the Normandy Bridge. As mentioned before, the von Karman spectrum is based on an assumption that the flow field is homogeneous and isotropic. Wind tunnel tests are obviously carried out in shear flow turbulence and the resulted turbulence is typically characterized by the Kaimal type spectra. However, this difference is perhaps negligibly small as shown in Figs.3.20 and 3.21.

4.3 Estimation of Sine Case Response

The biggest uncertainty in the calculation of sine case is the evaluation of aerodynamic force characteristics such as lift force, drag force and lift slope. These aerodynamic force coefficients greatly influence the root-mean-square response in both lateral and vertical bending motion. As mentioned in section 2.4.4, these parameters for the

sine case; i.e., the case of small aspect ratio, were taken from Winter's experimental results [52] on flat plates with small aspect ratio. For bridge models with box sections, these aerodynamic force coefficients could be considerably different from the flat plates. However, since there is no experimental results available for this case, the above assumption was introduced as the first approximation. It can be seen that the experimental evaluation of these aerodynamic force coefficients for sine cases could improve the agreement of analytical and test results.

Chapter 5
Conclusions and Comments

5.1 Conclusions

The effect of wind yawed angle on the buffeting response of cable-stayed bridges during their erection was emphasized as a major subject in the present study. The original modified buffeting analysis was only for the vertical bending vibration, although there is lateral buffeting observed experimentally . Therefore the study was extended to analyze lateral bending response under yawed wind. The comparison of analysis with test results is extended to actual cable-stayed bridge models.

It has been confirmed that the modified buffeting approach is effective in prediction of buffeting response of cable-stayed bridges during their erection. The conclusion of the study can be summarized as follows:

(1) The modified buffeting approach is further developed to predict lateral bending motion of cable-stayed bridges during their erection and the variation of wind directions is considered.

(2) The modified buffeting approach is applied to actual cable-stayed bridge models and proved effective. The buffeting analysis both in vertical mode and lateral mode is compared with the wind tunnel testing data for cable-stayed bridge models, and the calculated and experimental results are in general agreement.

(3) The analysis indicates that the buffeting response both in lateral and vertical bending oscillations is greater at high wind speed and is almost proportional to the intensity of turbulence. Wind tunnel tests confirmed this and the results agreed.

(4) When the effective wind velocity is normal to the bridge span (i.e. cosine case), the effect of aerodynamic damping on both vertical and lateral bending responses plays a principal role.

(5) When the effective wind velocity is parallel to a bridge model span (i.e. sine case), the effect of some additional lift caused by the vortices formed along the sides of the bridge model should be considered as well as aerodynamic damping. These aerodynamic force parameters include lift and drag force coefficients and lift slope. The variation of turbulence intensity along the bridge model span is also an important effect on lateral bending motion when wind direction is parallel to a bridge span.

5.2 Suggested Further Study

To obtain a better prediction of buffeting response under yawed wind, the present study has emphasized the importance of aerodynamic parameter evaluation. Wind tunnel testing is the most reliable way to find aerodynamically complicated behaviour.

Further study in prediction of buffeting response of cable-stayed bridges should include both theoretical analysis and wind tunnel testing. Additional study should investigate aerodynamic force behaviour for bridge models with box sections and small aspect ratio, i.e. in the case of wind parallel to the bridge span. Another study is needed to determine aerodynamic damping under yawed wind, not only for different bending oscillation but also for models with different cross-sections.

REFERENCES

1 Bisplinghoff, R. L., Ashley, H. and Halfman, R. L., Aeroelasticity, Addison-Wesley, 1955.

2 Barnard, R. H., " Wind loads on cantilevered roof structures", J. Wind Engineering and Industrial Aerodynamics Vol. 8, Nos. 1-2, pp. 21-30, July 1981.

3 Clough, R. W. and Penzien, J. , Dynamics of Structures, McGraw-Hill, 1975.

4 Curtiss, H.C. Jr., Scanlan, R.H. and Sisto, F., A Modern Course in Aeroelasticity, Dowell, E.H. ed., 2nd Ed., Kluwer Academic Publishers, Netherlands, 1989.

5 Damsgaard, A., "Wind tunnel tests for Kao Ping Hsi Bridge: Full model tests ----- construction condition and service condition", prepared for VCE - Vienna Consulting Engineers, DMI Report 92168, Danish Maritime Institute, 1993.

6 Davenport, A.G., " The response of slender line-like structures to a gust wind", Proc. ICE, Vol. 23, pp. 389-408, 1962.

7 Davenport, A.G., " Buffeting of a suspension bridge by storm wind", J. Structural Division, Proc. ASCE Vol. 88, No. ST3, pp. 233-268, 1962.

8 Davenport, A.G., " The use of taut strip models in the prediction of the response of long span bridges to turbulent wind", Proc. IUTAM/IAHR Symposium on Flow-Induced Structural Vibrations, Karlsluhe, Germany, 1972, Flow-Induced Structural Vibrations, E. Naudascher, ed., Springer-Verlag, Berlin, pp. 373-381, 1974.

9 Davenport, A.G., Isyumov, N., Fader, D.J. and Bowen, C.F.P., " A study of wind action on a suspension bridge during erection and on completion: the Narrows Bridge", Halifax, Nova Scotia, Canada, BLWT-3-69, University of Western Ontario, May 1969.

10 Davenport, A.G., Isyumov, N., Rothman, H. and Tanaka, H., " Wind induced response of suspension bridges - wind tunnel model and full scale observations", Proc. 5th Int. Conf. on Wind Engineering, Fort Collins, Colorado, July 1979, Cermak, J.E., ed., Pergamon Press, Oxford, U.K., Vol. 2, pp. 807-824, 1980.

11 Davenport, A.G. and King, J.P.C., " The incorporation of dynamic wind loads into the design specifications for long span bridges', Proc. ASCE Fall Convention & Structure Congress, New Orleans, Louisiana, pp. 1-30, October 1982.

12 Davenport, A.G. and King, J.P.C., " The influence of topography on the dynamic wind loading of long span bridges", J. Wind Engineering and Industrial Aerodynamics, Vol.

36, Nos. 1-3, Part2, pp. 1373-1382, 1990.

13 Farquharson, F.B., Smith, F.C. and Vincent, G.S. " Aerodynamic stability of suspension bridges with special reference to the Tacoma Narrows Bridge", University of Washington, Engineering Experiment, Station Bulletin No. 116, Parts I to V, 1950-1954.

14 Ferraro, V. and Irwin, P.A., " Recent experiences with aeroelastic wind tunnel studies of cable- stayed bridges ", Proc. Canada-Japan Workshop on Bridge Aerodynamics, National Research Council Canada, National Aeronautics Establishment, Ottawa, pp. 227-238, 1989.

15 Frazer, R.A. and Scruton, C., " A summarized account of the Seven Bridge aerodynamic investigation", National Physical Laboratory, NPL Aero. Report 222.

16 Gersten, K., " Calculation of non-linear aerodynamic stability derivatives of aeroplanes", Advisory Group for Aeronautical Research and Development, Report 342, April 1961.

17 Hinze, J.O., Turbulence, 2nd Ed., McGraw-Hill, New York, 1975.

18 Irwin, H.P.A.H., " Wind tunnel and analytical investigations of the response of Lions' Gate Bridge to a turbulent wind", National Research Council Canada, NAE-LTR-LA-210, 1977.

19 Irwin, P.A., " Prediction and control of the wind response of long-span bridges with plate girder decks", Proc. ASCE Structure Congress 1987, Orlando, Florida, pp. 268-280, August 1987.

20 Irwin, P.A., " Wind buffeting of cable-stayed bridge during construction", Proc. ASCE Structure Congress 1987, Orlando, Florida, pp. 164-177, August 1987.

21 Jancauskas, E.D. and Melbourne, W.H., " The aerodynamic admittance of two-dimensional rectangular section cylinders in smooth flow", J. Wind Engineering and Industrial Aerodynamics, Vol. 23, pp. 395-408, July 1986.

22 Kaimal, J.C., Wyngaard, J.C, Izumi, Y. and Coté, O.R., "Spectral characteristics of surface layer turbulence", Quart. J. Royal Met. Soc., Vol. 98, pp. 563-589, 1972.

23 Kimura, K. and Tanaka, H., " Bridge buffeting due to wind with yaw angles", J. Wind Engineering and Industrial Aerodynamics, 41-44 pp.1309-1320, 1992.

24 Kimura, K. " Flat plate buffeting in yawed wind with possible application to bridges", PhD thesis, University of Ottawa, Ottawa, Ontario, Canada, 1991.

25 Larose, G. L. and Livesey, F. M., " Wind -tunnel study of the Pont de Normandie during construction: Model design report & Aeroelastic model tests", Prepared for Monberg & Thorsen A/S, DMI Reports 92159.01 and 92159.03, Danish Maritime Institute, June 1993.

26 Leonhardt, F. and Zellner, W., " Past, present and future of cable-stayed bridges", Cable-Stayed Bridges, Recent Developments and their Future, M. Ito, Y.Fujino, T. Miyata and N. Narita eds., Elsevier, 1991, pp. 1-34.

27 McCormick, B.W., Aerodynamic, Aeronautics, and Flight Mechanics, John Wiley & Sons, New York, 1979.

28 Melbourne, W.H., " Model and full scale response to wind action of the cable stayed box girder West Gate Bridge", Practical Experiences with Flow-Induced Vibrations, E. Naudascher and D. Rockwell, eds., Springer- Verlag, Berlin, pp. 625-632, 1980.

29 Melbourne, W.H. and Cheung, J.C.K., " Reducing the wind loading on large cantilevered roofs", Proc. 7th Int. Conf. on Wind Engineering, Part 1, Aachen, Germany, July 1987, J. Wind Engineering and Industrial Aerodynamics, Vol. 28, Nos. 1-3, pp. 401-410, August 1988.

30 Scanlan, R.H. and Tomko, J.J., " Airfoil and bridge deck flutter derivatives", J. Eng. Mech. Div., ASCE (97), EM6, 1971, pp. 1717-1737.

31 Scanlan, R.H., " The action of flexible bridges under wind, II: buffeting theory", J. Sound and Vibration, Vol. 60, No. 2, pp. 201-211, 1978.

32 Scanlan, R.H., " On the state of stability considerations for suspended-span bridges under wind", Practical Experiences with Flow-Induced Vibrations, E.Naudascher and D.Rockwell, Eds., Spring-Verlag, Berlin, pp. 595-618, 1980.

33 Scanlan, R.H., " Role of indicial functions in buffeting analysis of bridges", J. Structural Engineering, Vol. 113, No. 4, ASCE, pp. 555-575, April 1987.

34 Scanlan, R.H., " Bridge buffeting by skew winds in erection stages", Proc. ASCE (119) EM2, February 1993, pp.251-269.

35 Schlichting, H. and Truckenbrodt, E.,Aerodynamics of the Airplane, McGraw-Hill, New York, 1979.

36 Scruton, C., "Experiments on the aerodynamic stability of suspension bridges ", National Physical Laboratory, NPL Aero Report 185 and 189, 1951.

37 Sears, N.R., " Some aspects of stationary aerofoil theory", J. Aeronant. Sc. (8) 2, 1941, pp. 104-108.

38 Simiu, E. and Scanlan, R.H., Wind Effects on Structures, 2nd Ed., John Wiley & Sons, New York, 1985.

39 Sockel, H., " Fundamentals of wind engineering", Wind-Excited Vibrations of Structures, H. Sockel, ed., Springer-Verlag, 1994, pp. 85-160.

40 Tanaka, H. and Davenport, A.G., " Response of taut strip models to turbulent wind", J. Engineering Mechanics, Proc. ASCE, Vol. 108, No. EM1, pp. 33-49, February 1982.

41 Tanaka, H. and Davenport, A.G., " Wind-induced response of Golden Gate Bridge", J. Engineering Mechanics, Vol. 109, No. 1, ASCE, pp.296-312, February 1983.

42 Tanaka, H., " On wind tunnel testing of taut strip bridge models ", Proc. 3rd US-Japan Workshop on Bridge Engineering, Tsukuba, Japan, pp.318-323, May 1987.

43 Tanaka, H., " Similitude and modelling in wind tunnel testing of bridges ", Bluff Body Aerodynamics and Its Applications, M. Ito, M. Matsumoto and N. Shiraishi eds., Elsevier,1990, pp. 283-300.

44 Tanaka, H. and Larose, G. L., " Wind tunnel tests of cable-stayed bridges at their erection stage and effects of wind yaw angles", Proc. Int. Seminar on Utilization of Large Boundary Wind Tunnels, Tsukuba, Japan,1993, pp. 141-162.

45 Virlogeux, M., " Wind design and analysis for the Normandy Bridge", Proc. of Symposium on Aerodynamics of Large Bridges, Copenhagen, Denmark, Feb. 1992, pp. 183-216.

46 von Karman, T., " Progress in the statistical theory of turbulence", Proc. of the National Academy of Science, Washington, D.C., 1948, pp. 530-539.

47 Wardlaw, R.L., " Wind effects on bridges", Bluff Body Aerodynamics and Its Applications, M.Ito, M. Matsumoto and N. Shiraishi eds., Elsevier Science Publisher B.V., 1990, pp. 301-312.

48 Wardlaw, R.L., Tanaka, H. and Utsunomiya, H., " Wind tunnel experiments on the effect of turbulence on the aerodynamic behaviour of bridge road decks", J. Wind Engineering and Industrial Aerodynamics, Vol. 14, Nos. 1-3, pp. 247-257, December 1983.

49 Wardlaw, R.L., " Some observations the effects of turbulence on the aerodynamic stability of bridge road decks", Bridge Aerodynamics, T.T. L., London 1981. pp. 73-76.

50 Wardlaw, R. L., " Cable supported bridges under wind action", Cable-Stayed Bridges, Recent Developments and their Future, M. Ito, Y. Fujino, T. Miyata and N. Narita, eds.,Elsevier, 1991, pp. 213-234.

51 Wyatt, T.A., " The dynamic behaviour of cable-stayed bridges: Fundamentals and parametric studies", Cable -Stayed Bridges, Recent Developments and their Future, M. Ito, Y.,Fujino, T. Miyata and N. Narita, eds., Elsevier, 1991, pp. 151-170.

52 Winter, H., " Flow phenomena on plates and airfoils of short span", National Advisory Committee for Aeronautics, Technical Memorandum No. 798, July 1936.

53 Xie, J., Tanaka, H., Wardlaw, R.L. and Savage, M.G., " Buffeting analysis of long span bridges to turbulent wind with yaw angle", J. Wind Engineering and Industrial Aerodynamics, Vol. 37, No. 1, pp. 65-77, February 1991.

54 Zan, S. J., " The effect of mass, wind angle and erection technique on the aeroelastic behaviour of a cable-stayed bridge model", National Research Council Canada, NAE-AN-46, September 1987.

55 Zan, S. J., " Wind tunnel investigation of the wind-induced response of the Roosevelt Lake Steel Arch Bridge using an aeroelastic model", National Research Council Canada, NAE-LTR-LA-306, October 1987.

56 Zan, S. J., Yamada, H. and Tanaka, H., " The influence of turbulence and deck section geometry on the aeroelastic behaviour of a cable-stayed bridge model", National Research Council Canada, NAE-AN-40, August 1986.

57 Wind Loading and Wind-Induced Structural Response, A state-of-the-art report prepared by the Committee on Wind Effects, ASCE, 1987.

Figures

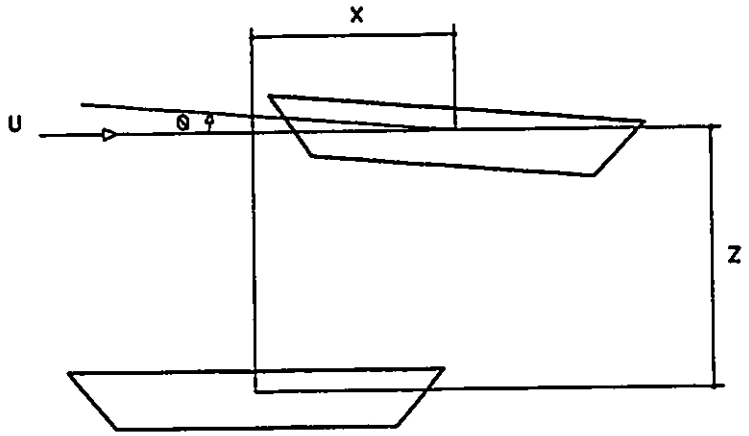

Fig. 2.1 Degrees of freedom for buffeting analysis

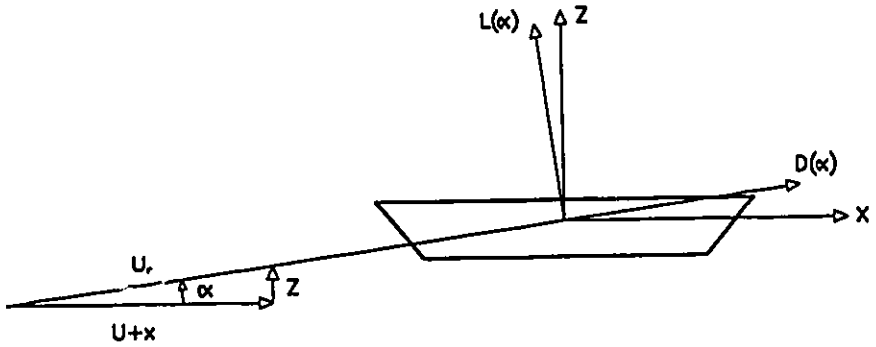

Fig. 2.2 Quasi-steady aerodynamic forces by the bridge deck motion

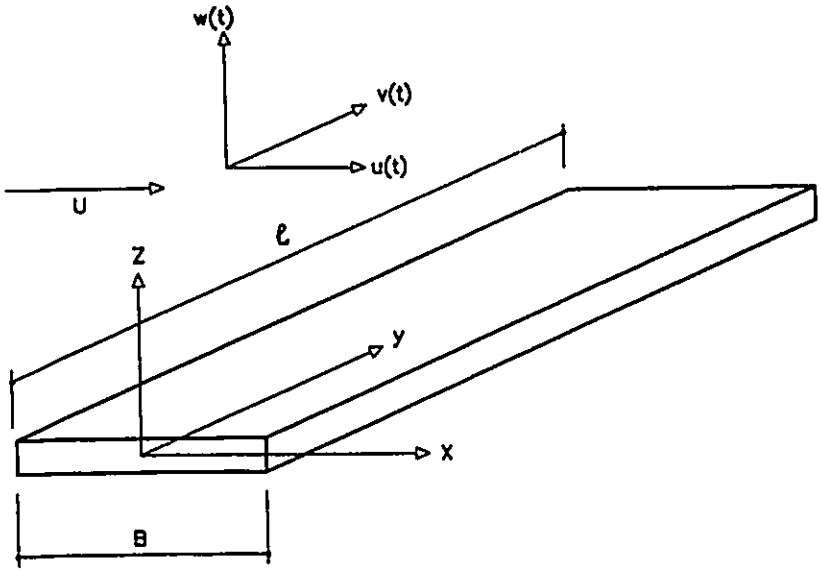

Fig. 2.3 A line-like structure

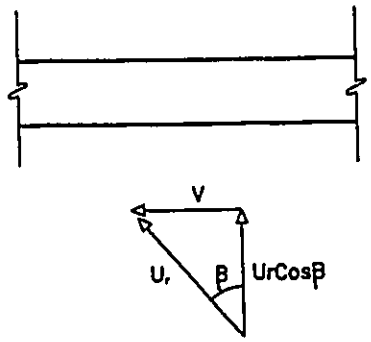

Fig. 2.4 A moving infinitely long plate

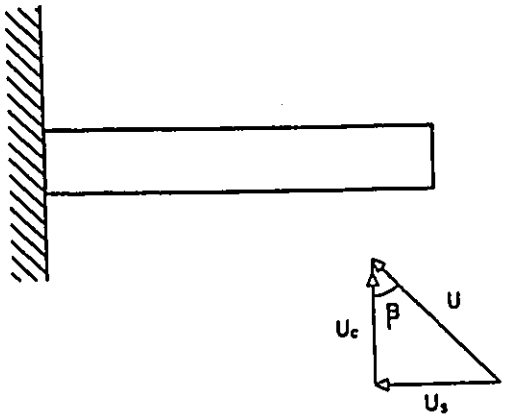

Fig. 2.5 Effective wind speeds for two leading edges

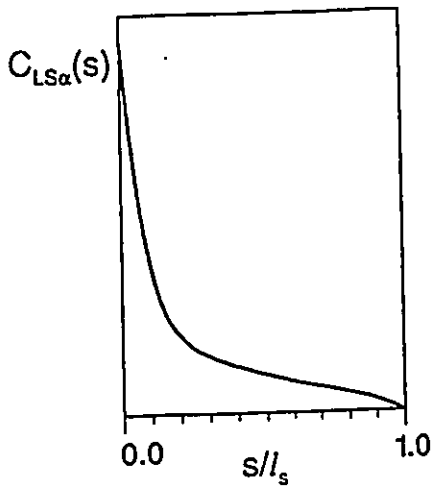

Fig. 2.6 Slope of $C_{L\alpha}(s)$

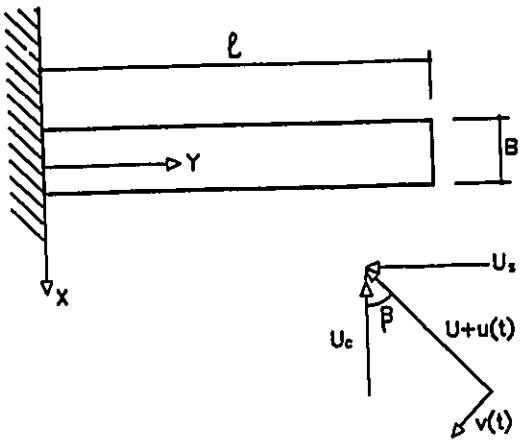

Fig. 2.7 A cantilever deck under lateral buffeting force

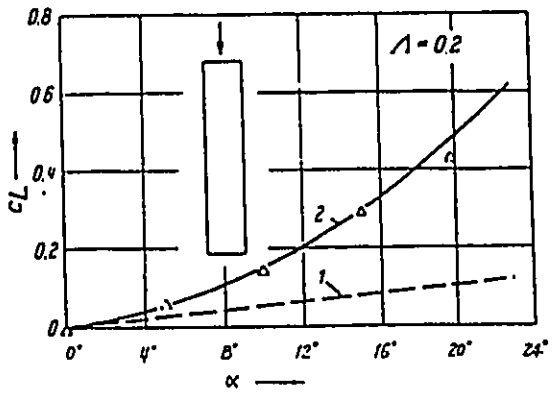

curve 1, linear theory, curve 2, nonlinear theory

Fig. 2.8 Lift coefficients vs. angle of attack

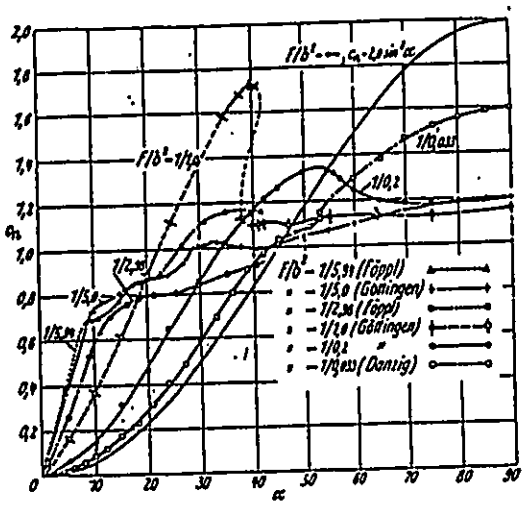

Fig. 2.9 Normal force coefficients C_n for flat rectangular plates

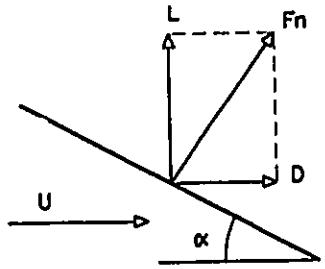

Fig. 2.10 Flat plate under wind loading

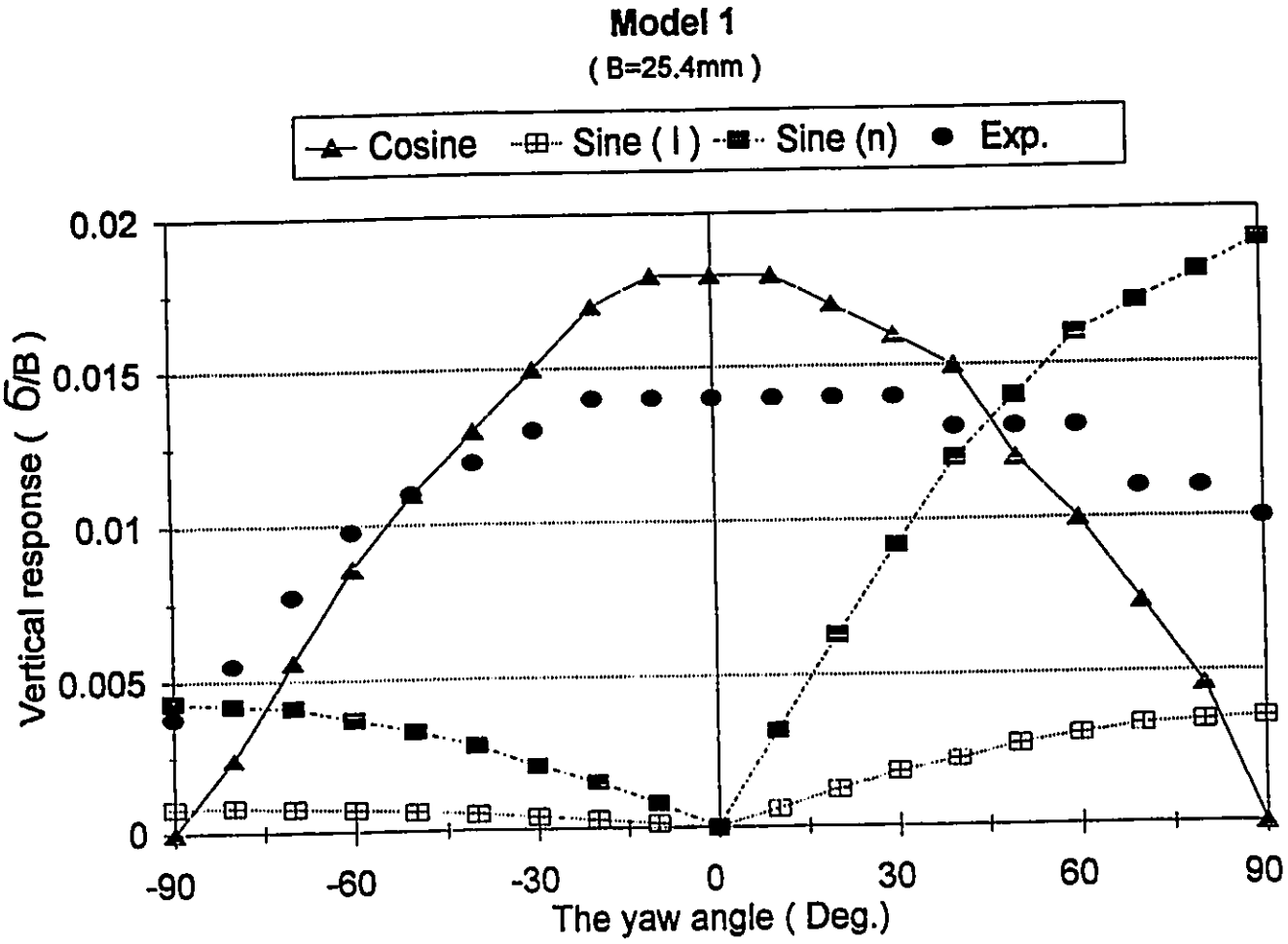

Fig. 3.1 Buffeting response for flat plate (Model 1)

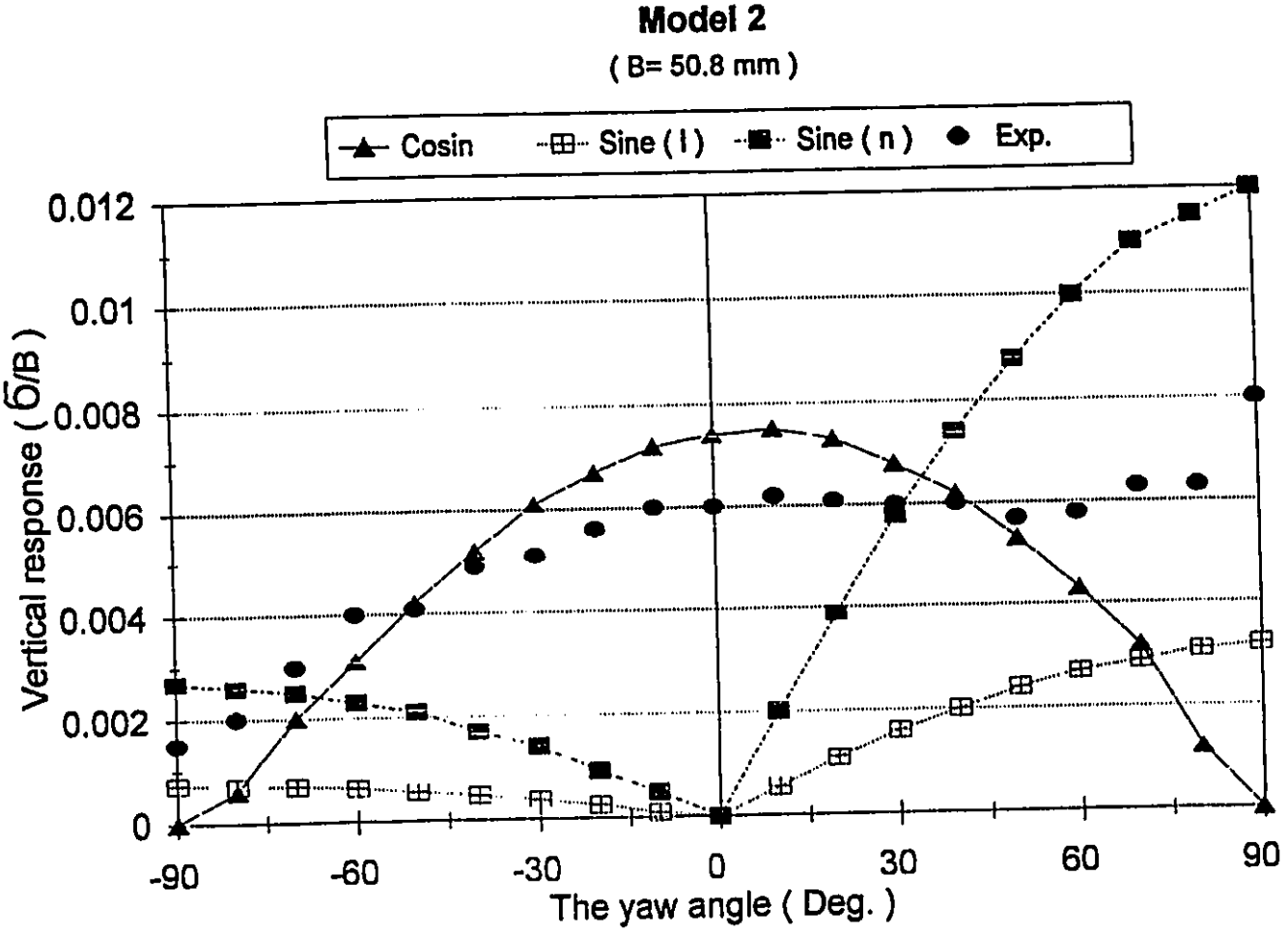

Fig. 3.2 Buffeting response for flat plate (Model 2)

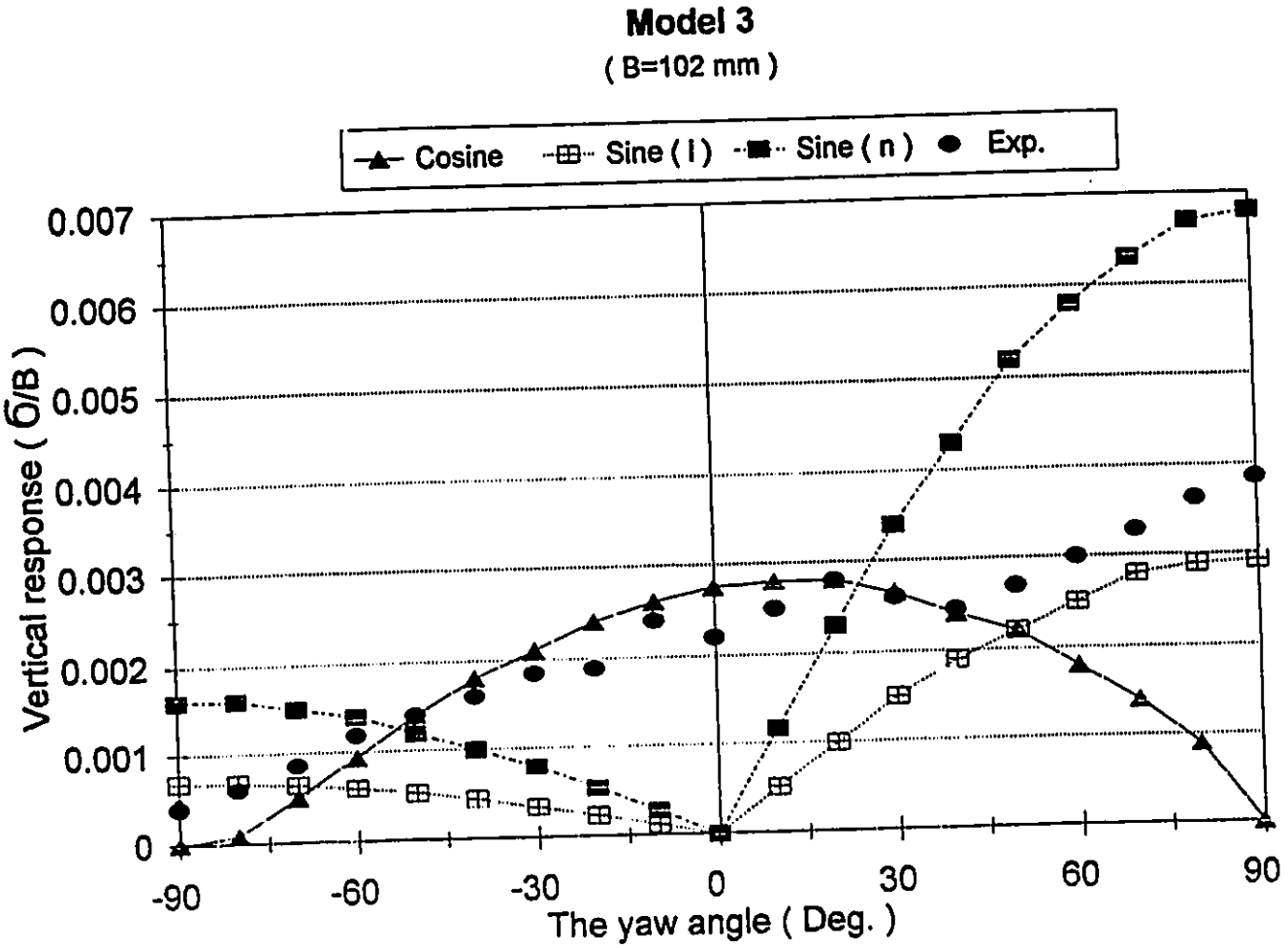

Fig. 3.3 Buffeting response for flat plate (Model 3)

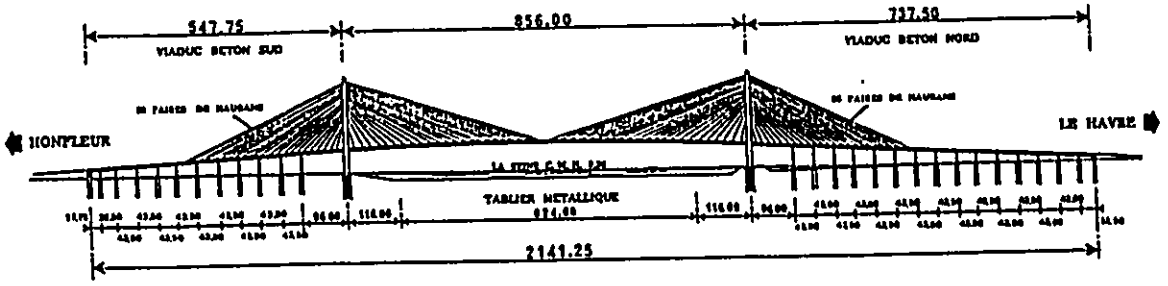

Fig. 3.4 Prototype dimensions of the Normandy Bridge

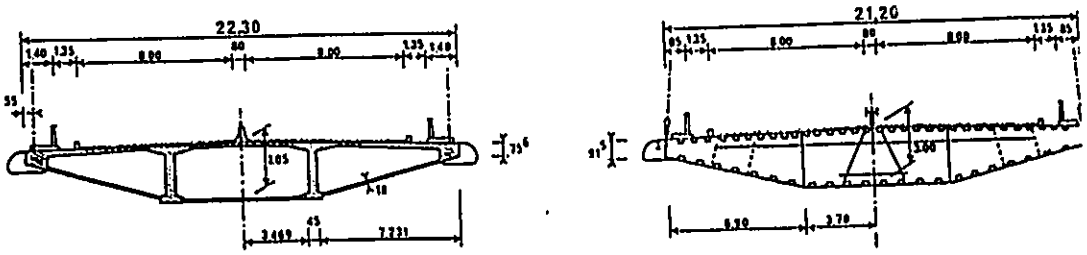

Fig. 3.5 Cross-sections of the Normandy Bridge, respectively of the concrete deck and steel deck.

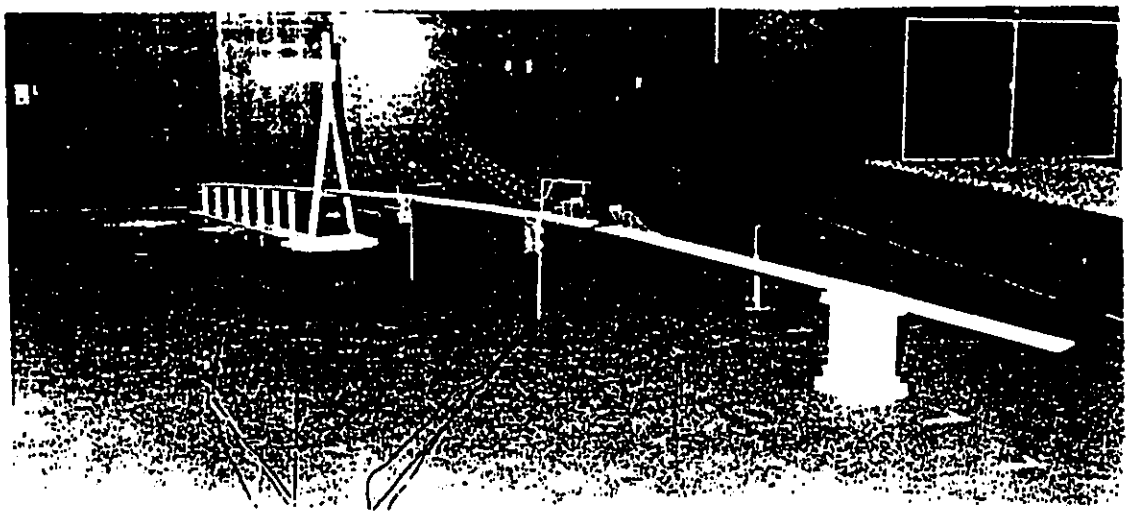

Fig. 3.6 Photograph of the aeroelastic model of the Normandy Bridge

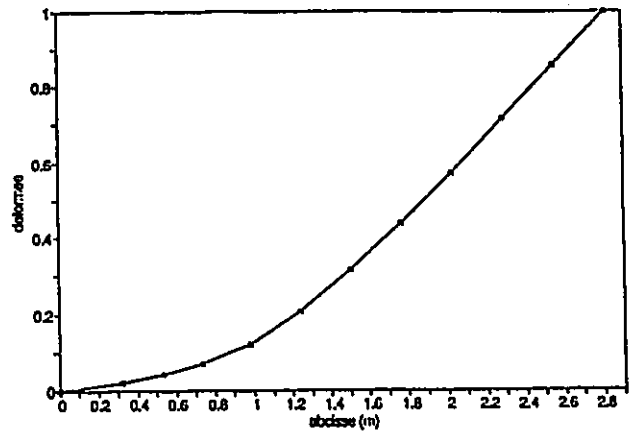

Fig. 3.7 The first lateral mode shape of the Normandy bridge model

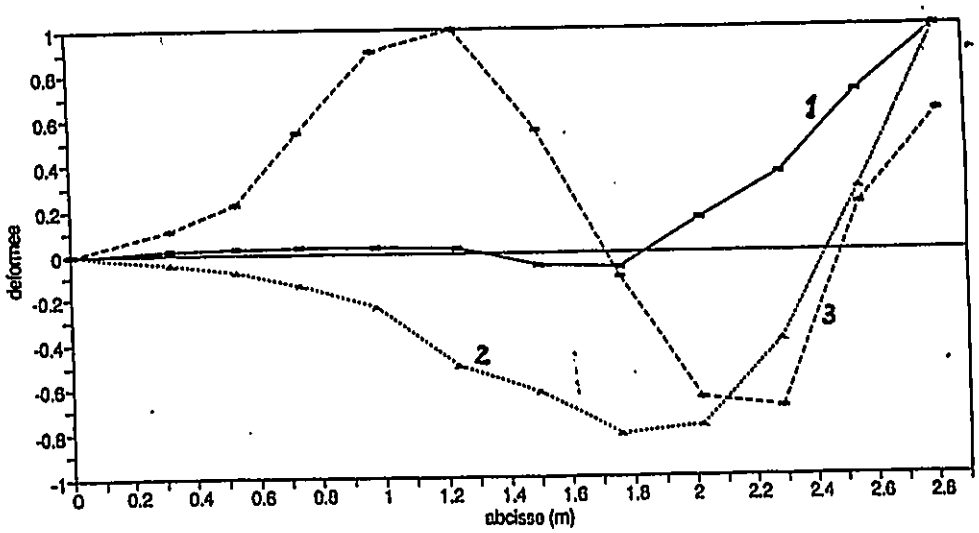

Fig. 3.8 The vertical mode shapes of the Normandy Bridge model

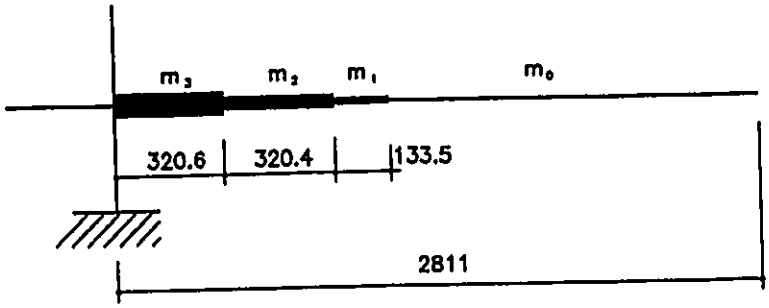

$m_0 = 0.443$
$m_1 = 1.73$
$m_2 = 2.09$
$m_3 = 2.35$

Fig. 3.9 Dimensions and mass distribution of the Normandy Bridge model
unit: length (mm), mass (Kg /m)

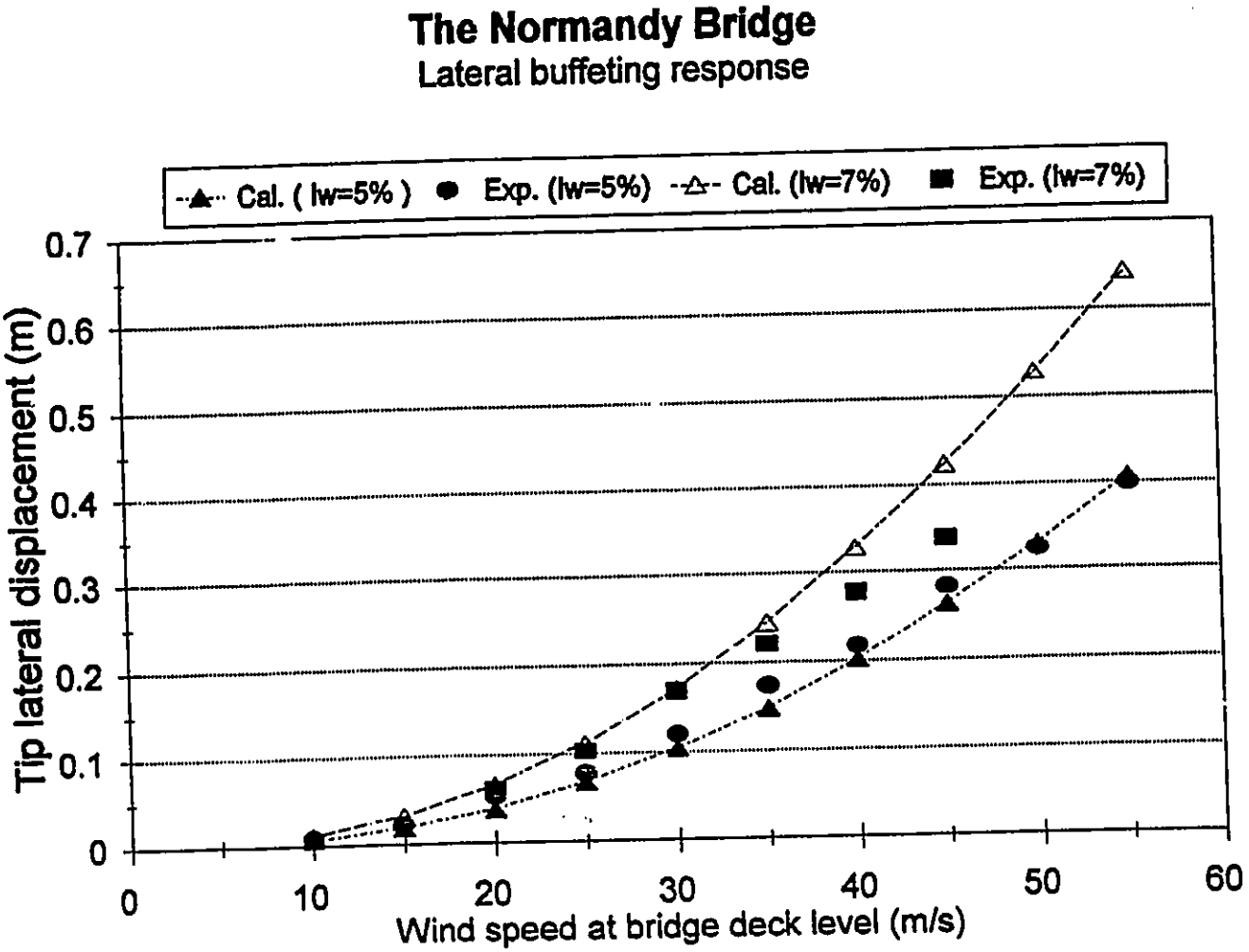

Fig. 3.10 Lateral displacement at the cantilever tip vs. wind speed

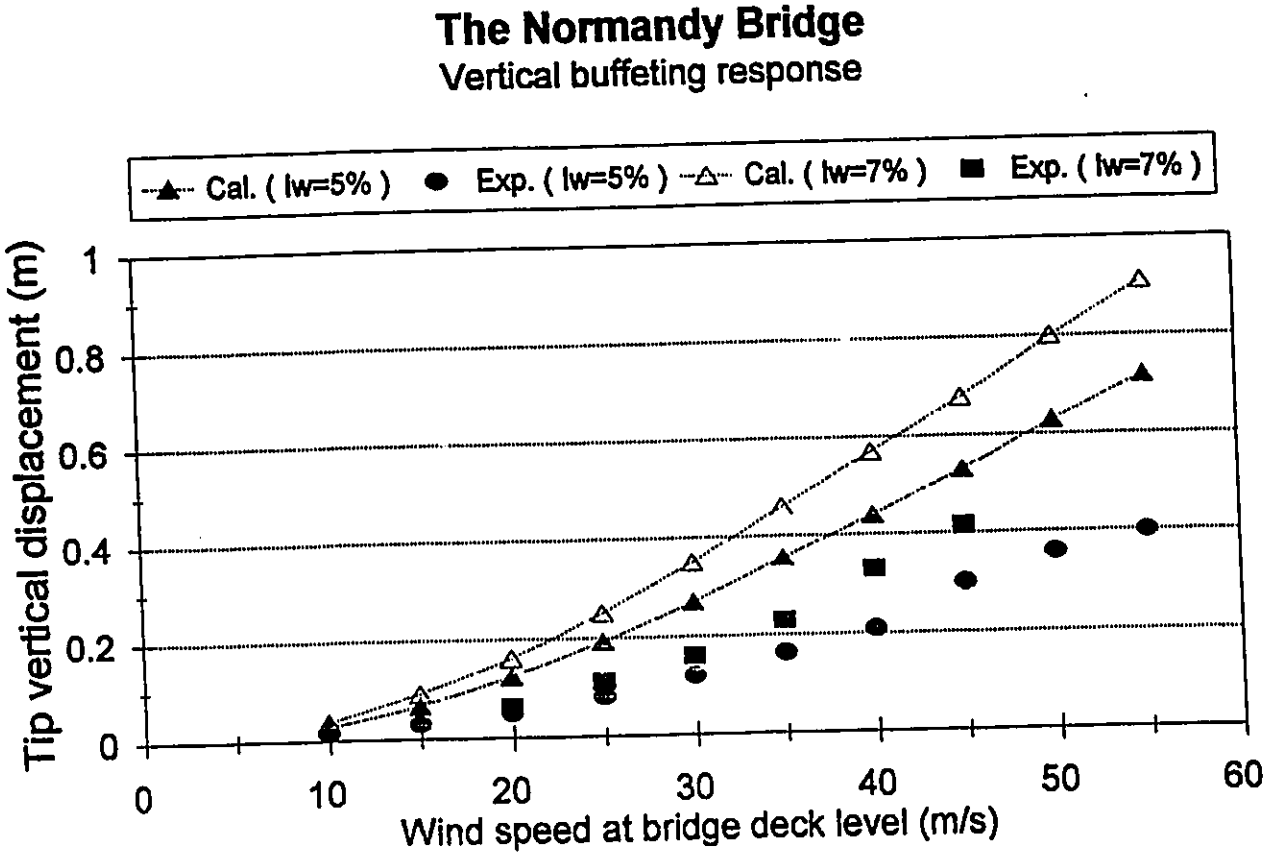

Fig. 3.11 Vertical displacement at the cantilever tip vs. wind speed

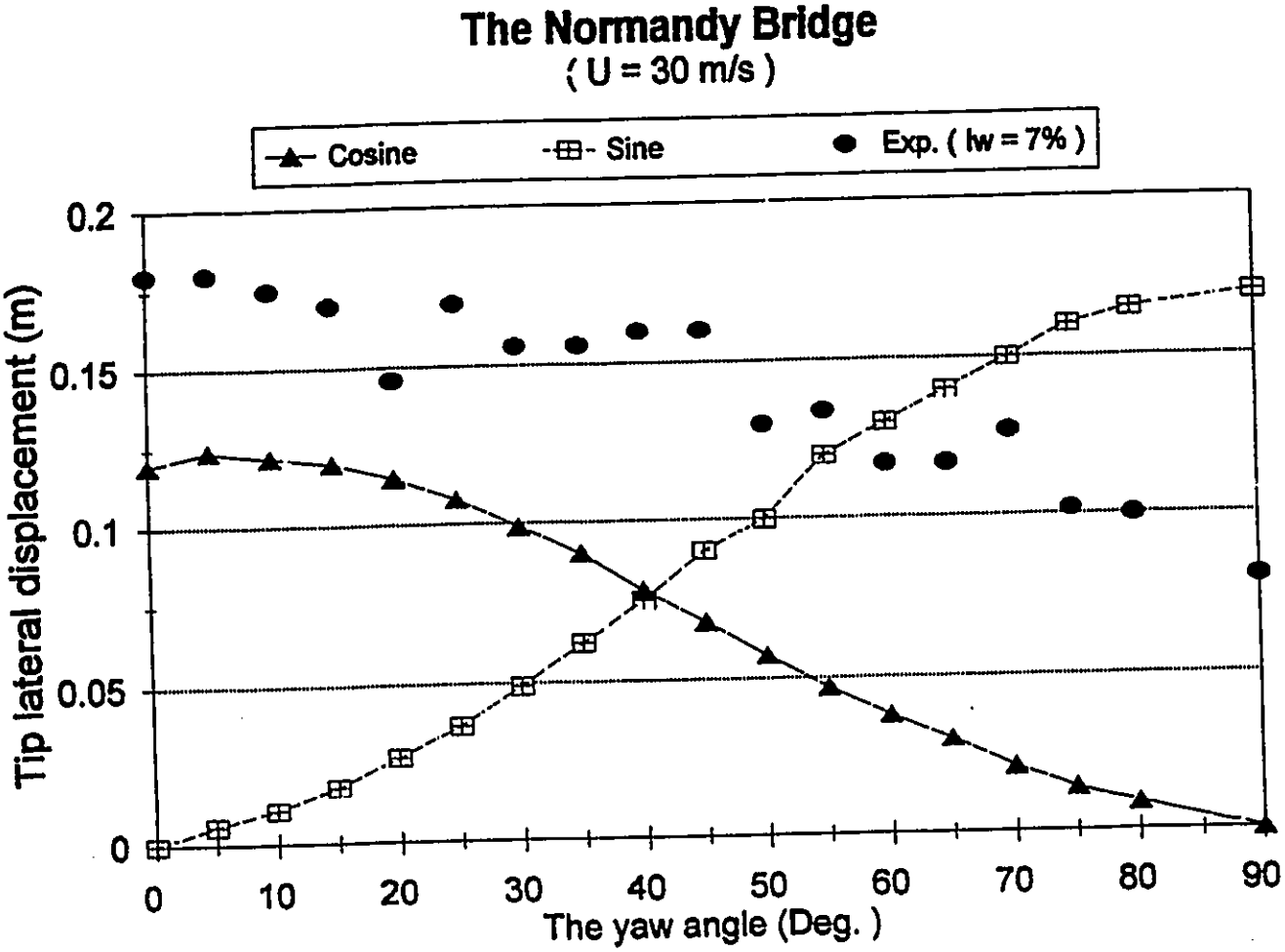

Fig. 3.12 Lateral response vs. yaw angle (U = 30 m/s)

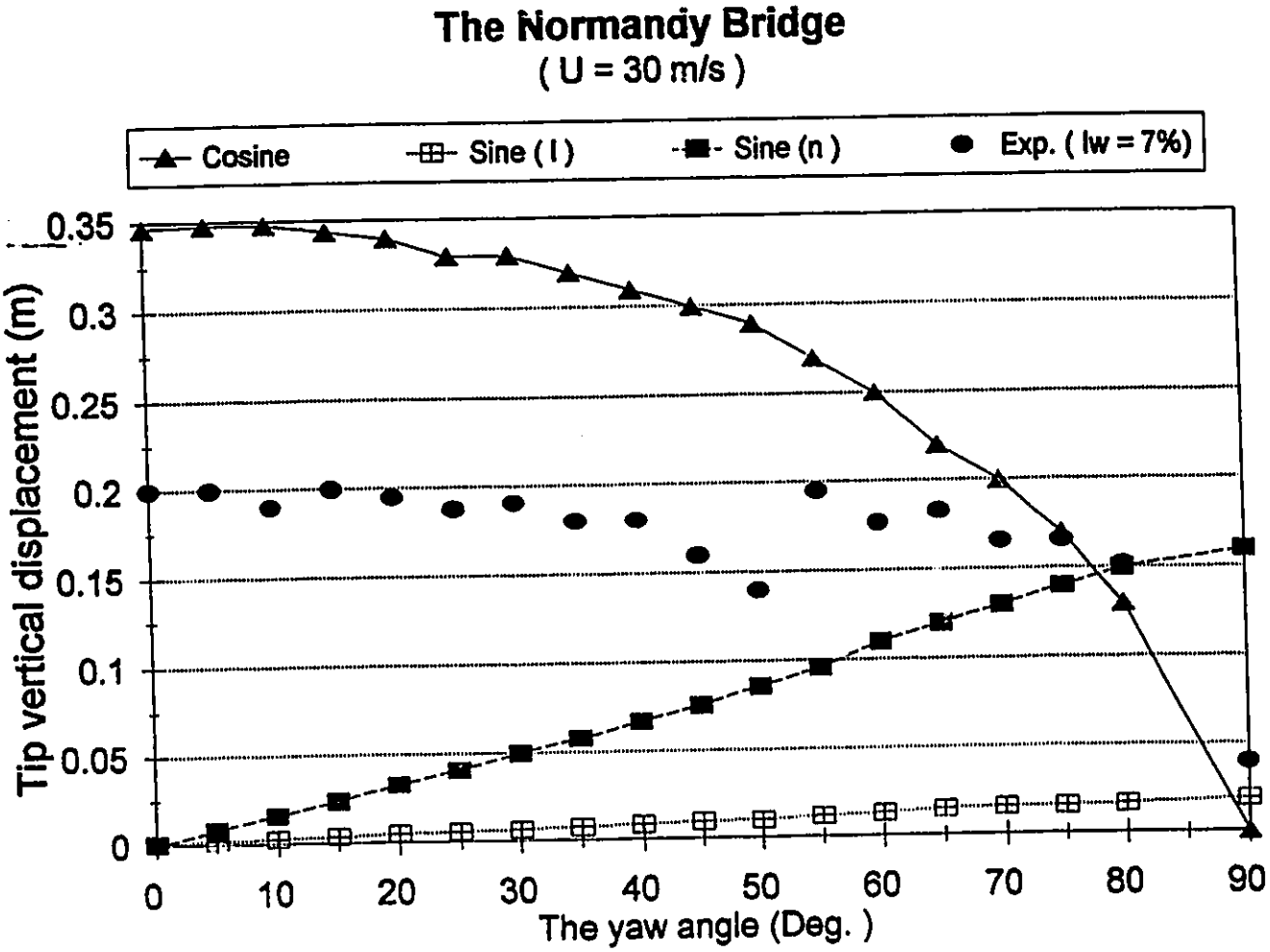

Fig. 3.13 Vertical response vs. yaw angle (U = 30 m/s)

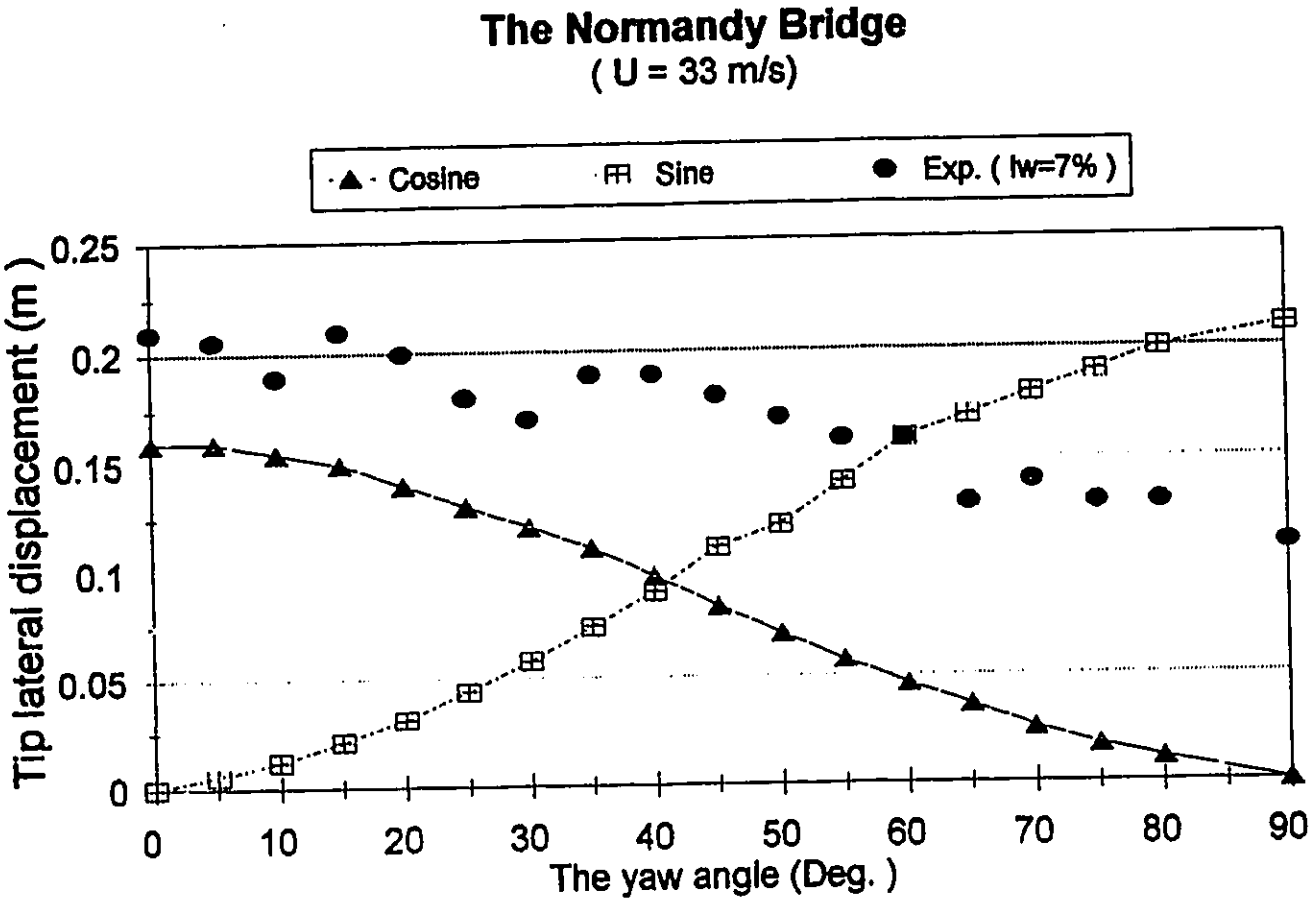

Fig. 3.14 Lateral response vs. yaw angle (U= 33 m/s)

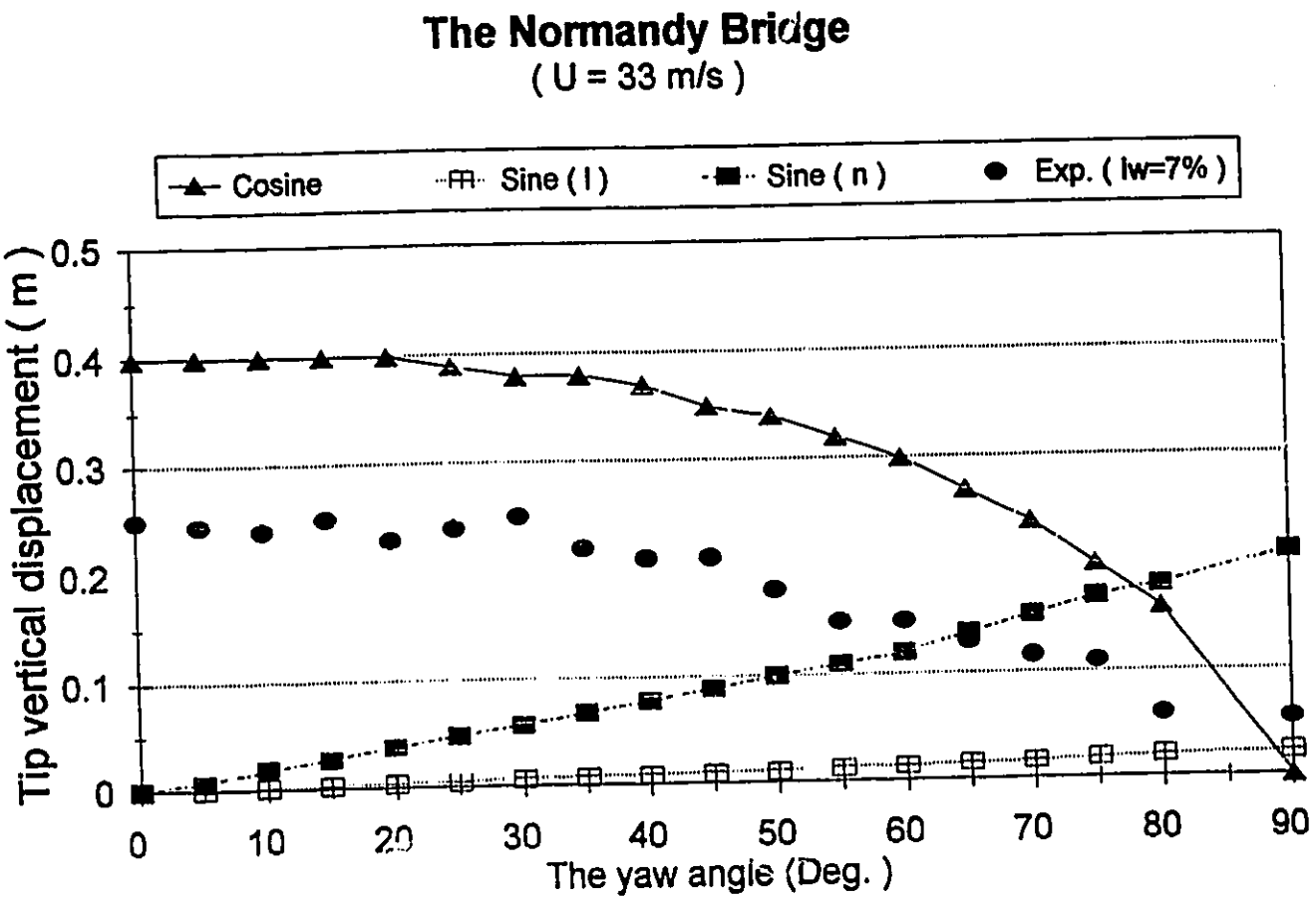

Fig. 3.15 Vertical response vs. yaw angle (U = 33 m / s)

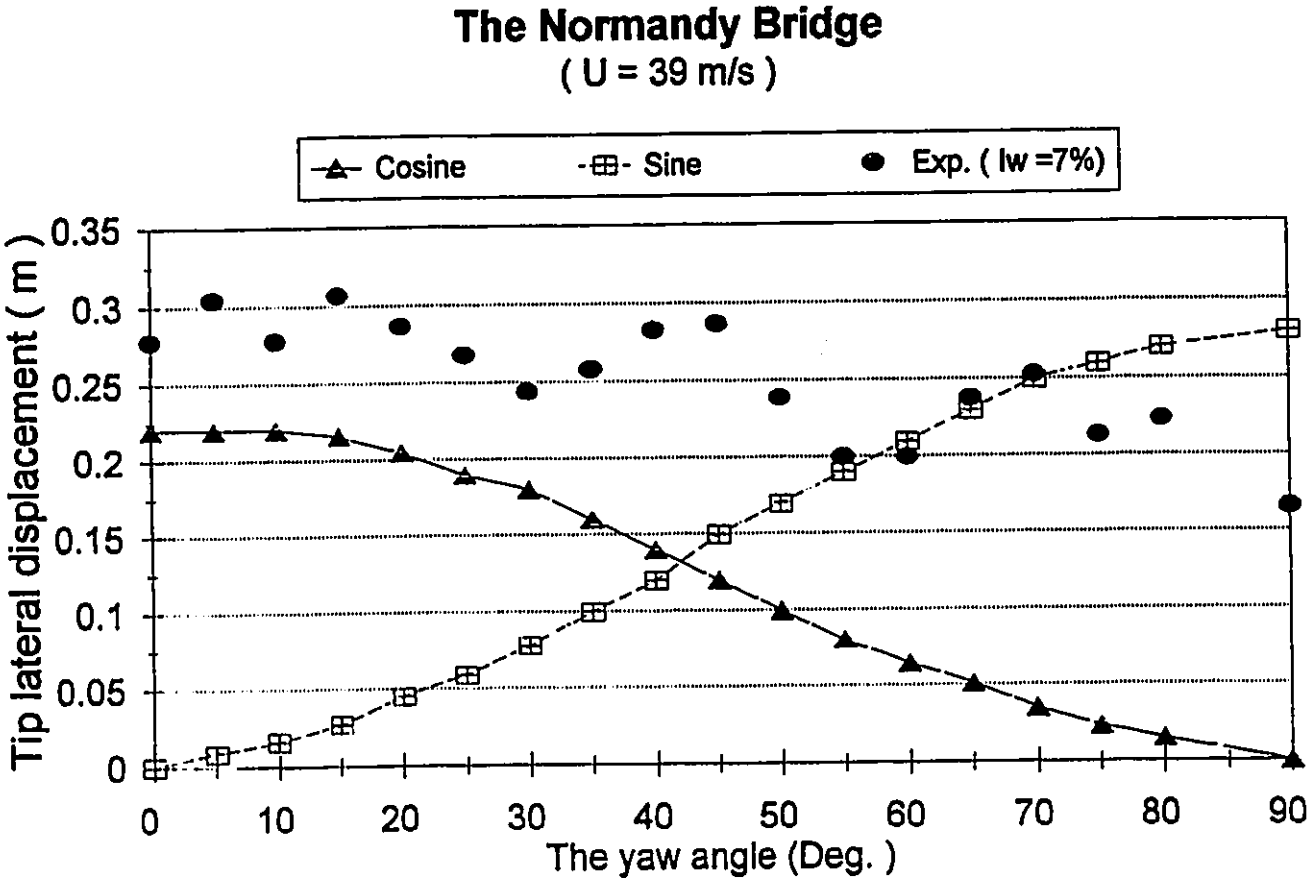

Fig. 3.16 Lateral response vs. yaw angle (U = 39 m / s)

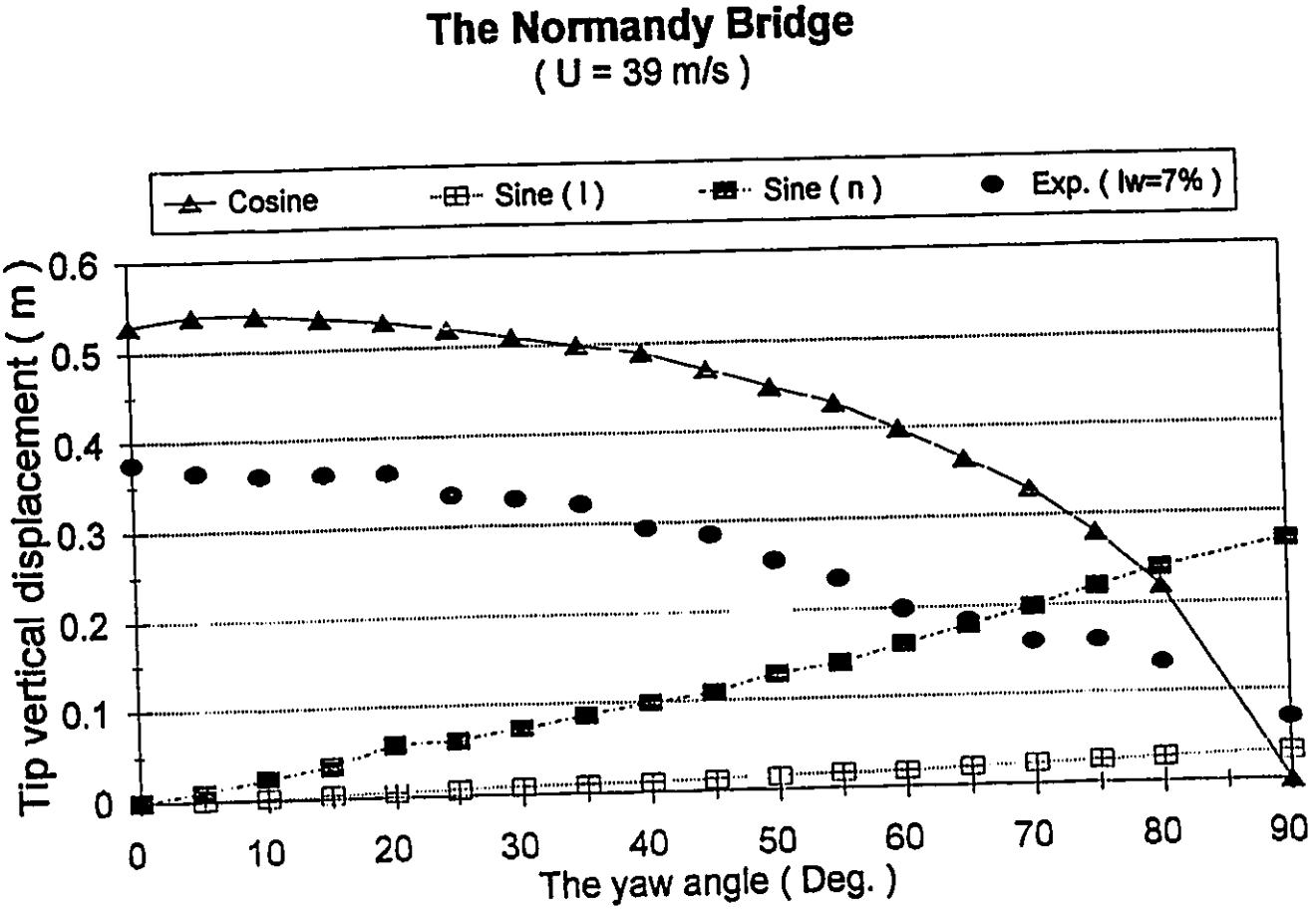

Fig. 3.17 Vertical response vs. yaw angle (U = 39 m/s)

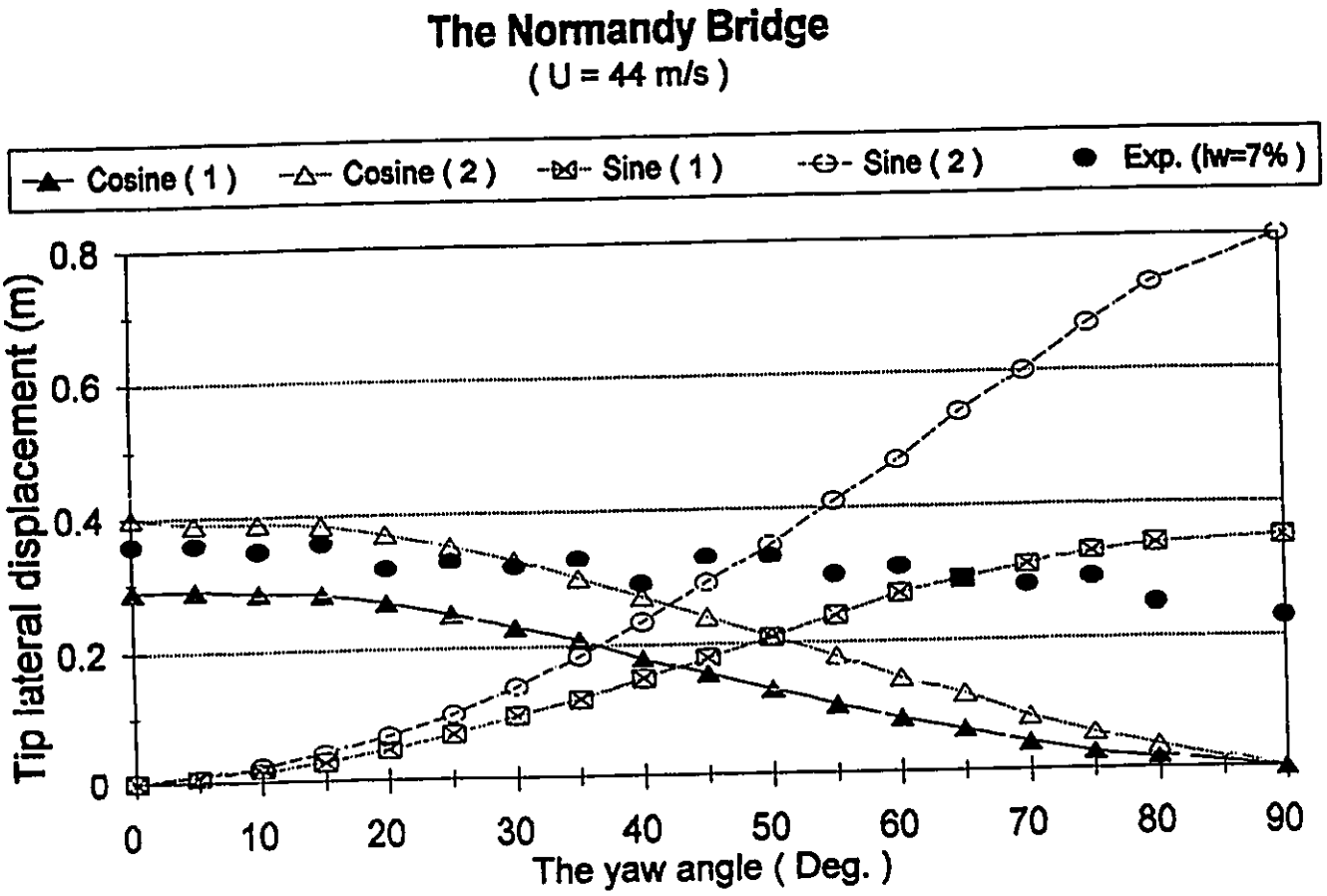

Fig. 3.18 Lateral response vs. yaw angle (U = 44 m/s)

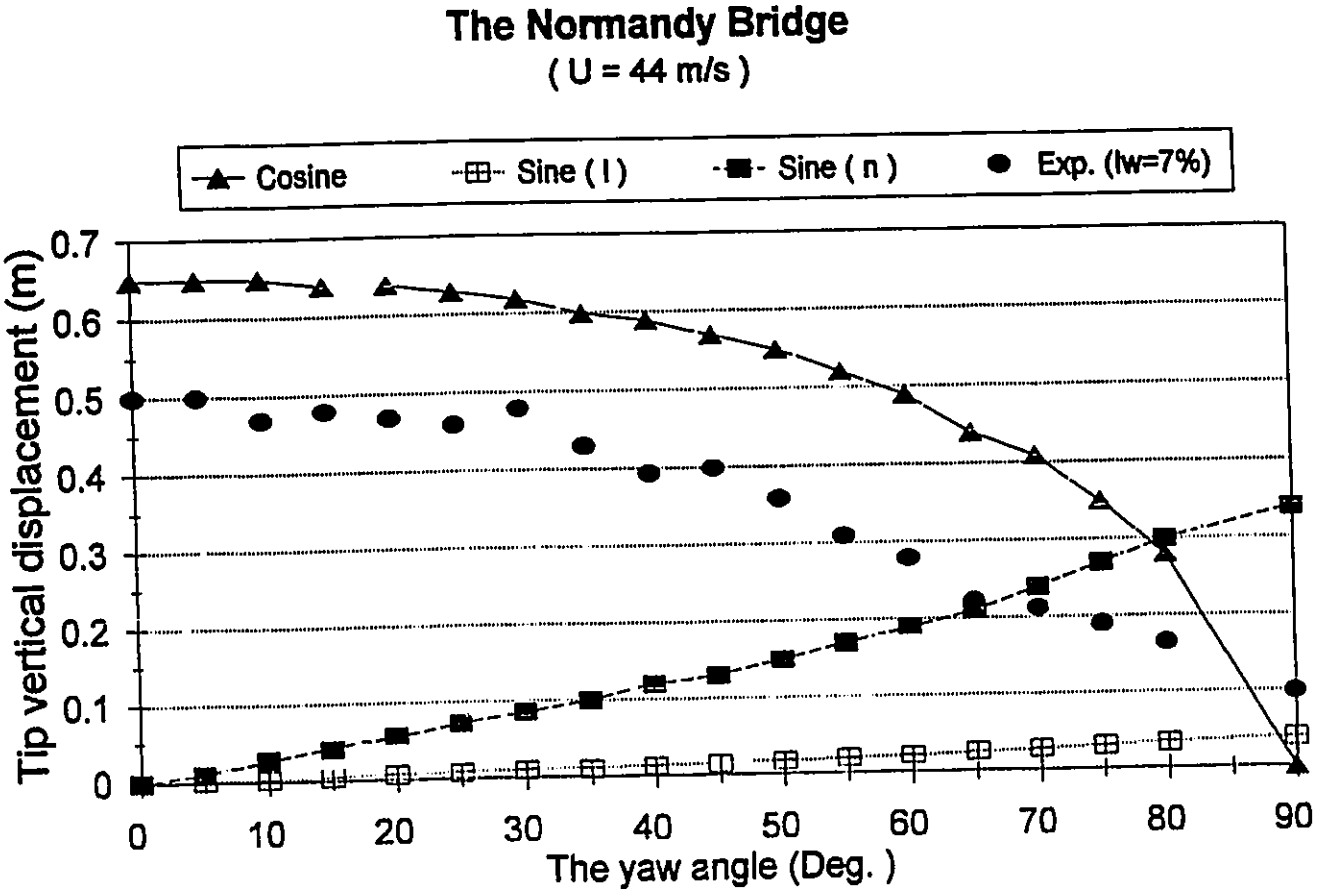

Fig. 3.19 Vertical response vs. yaw angle (U = 44 m/s)

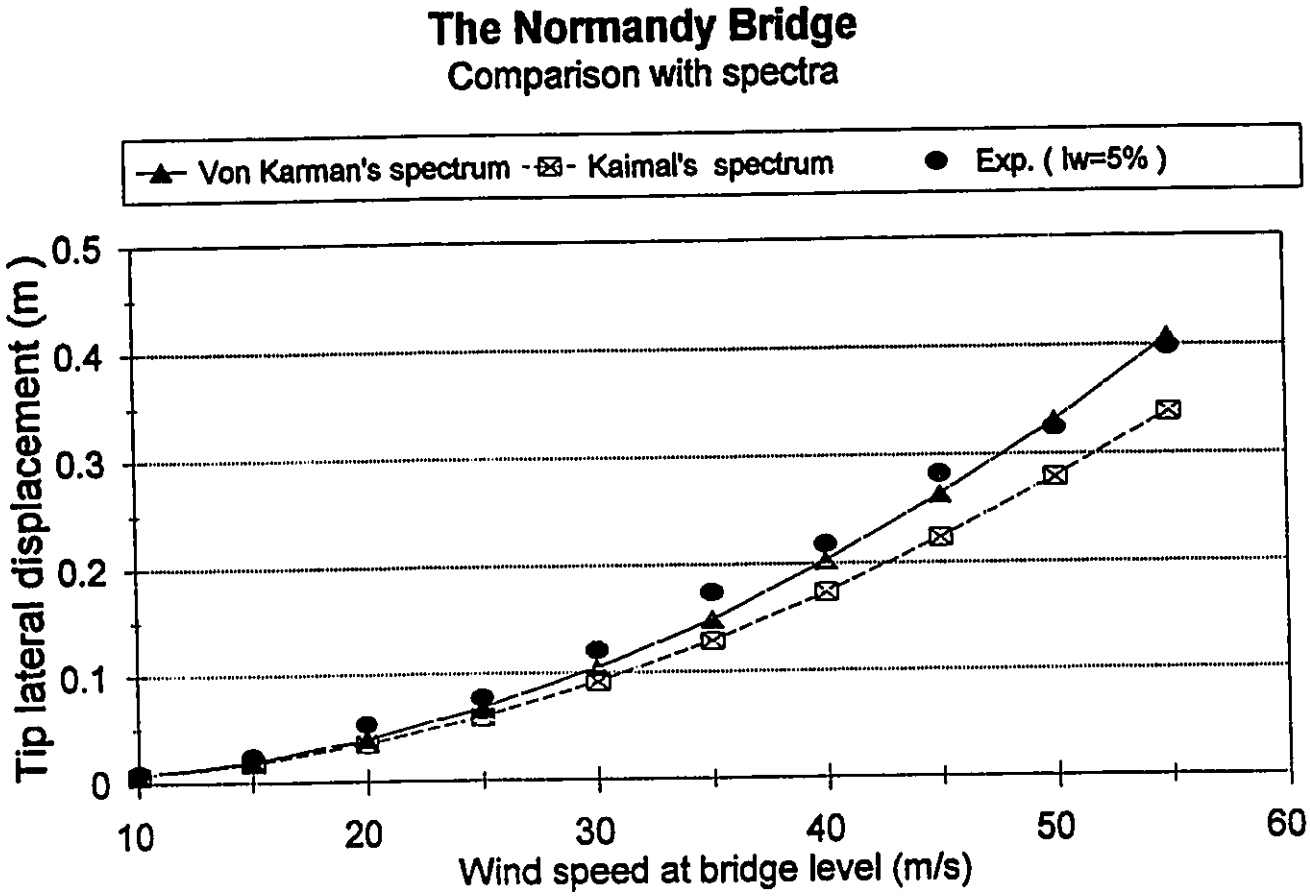

Fig. 3.20 Lateral response using Karman's and Kaimal's spectra

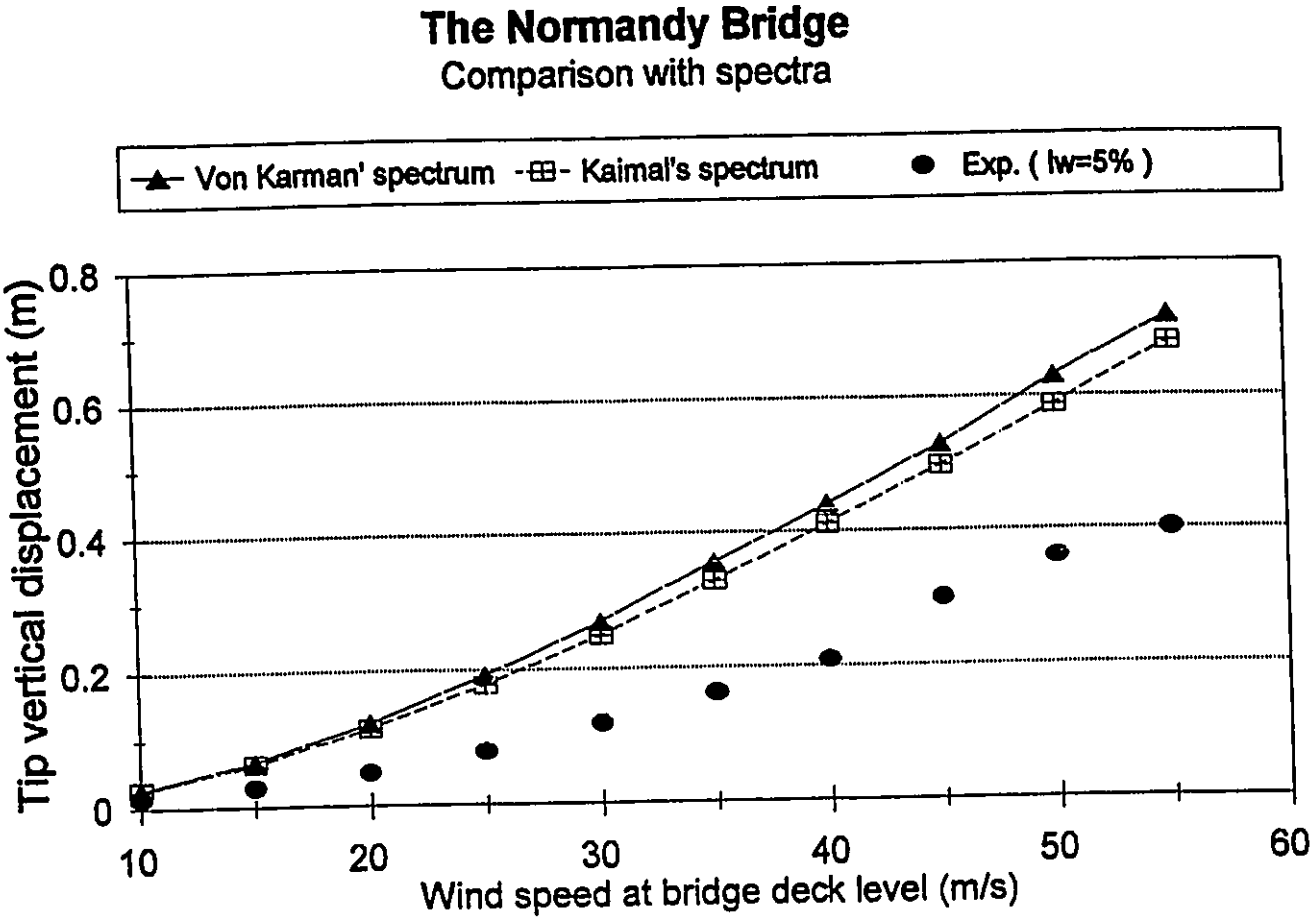

Fig. 3.21 Vertical response using Karman's and Kaimal's spectra

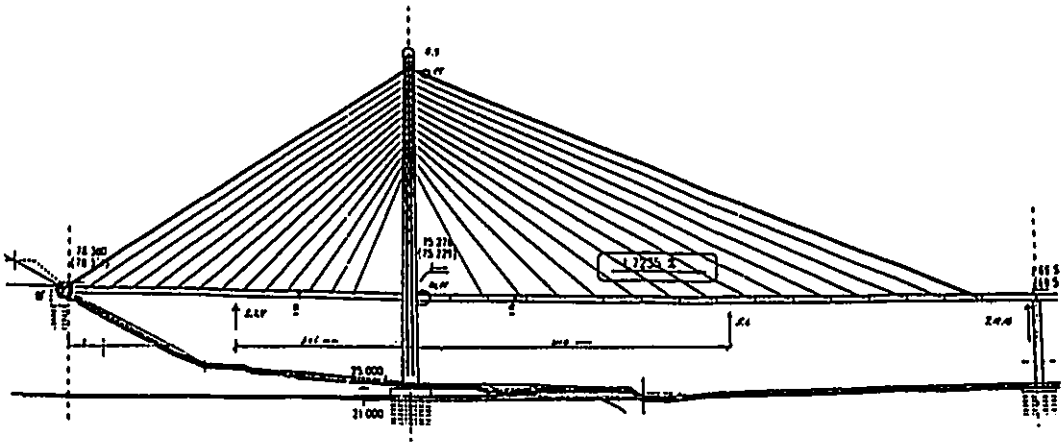

Fig. 3.22 General configuration of the Kao Ping Hsi Bridge

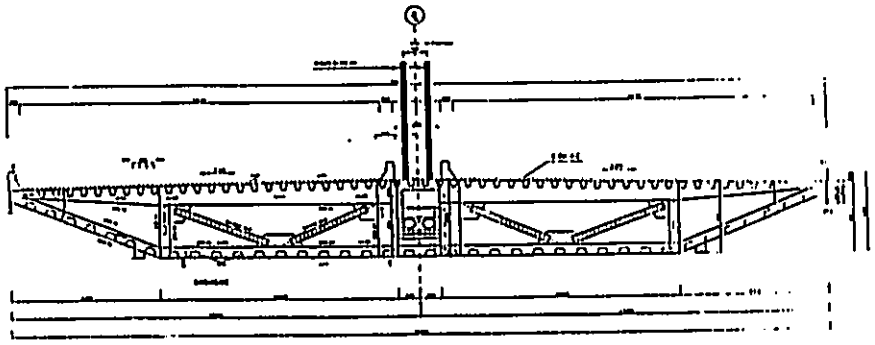

Fig. 3.23 Cross-section of the Kao Ping Hsi Bridge

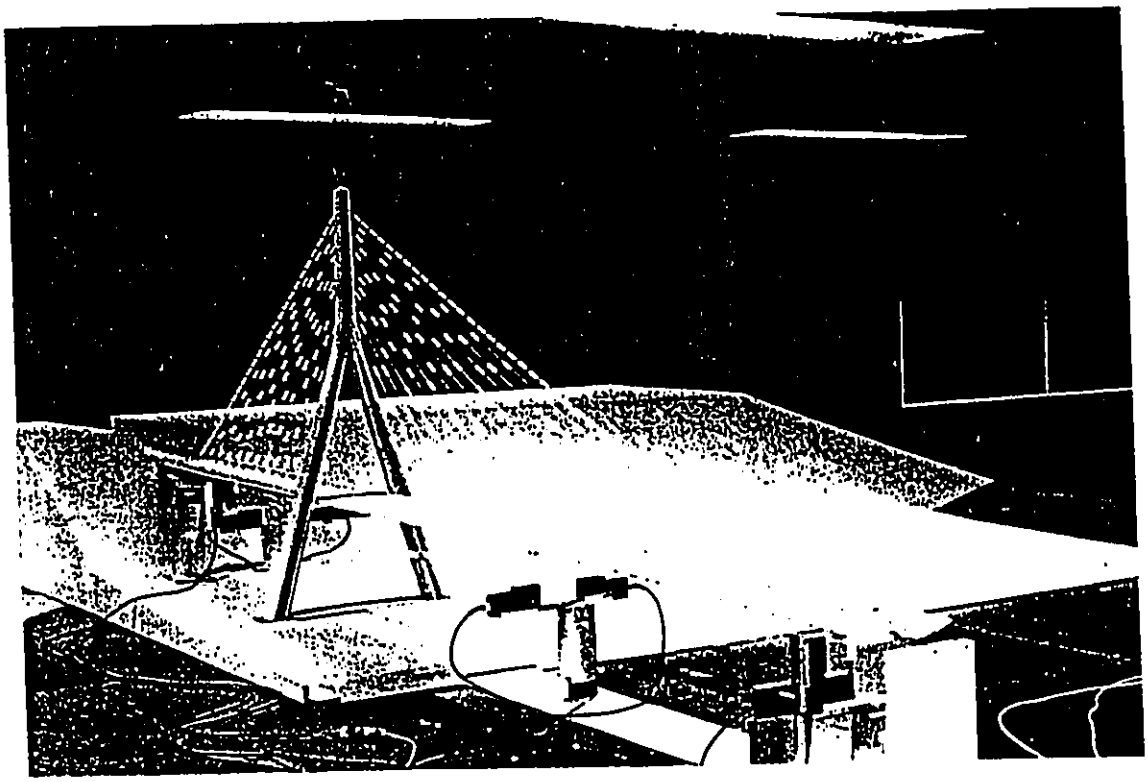

Fig. 3.24 Photograph of the aeroelastic model of the Kao Ping Hsi Bridge

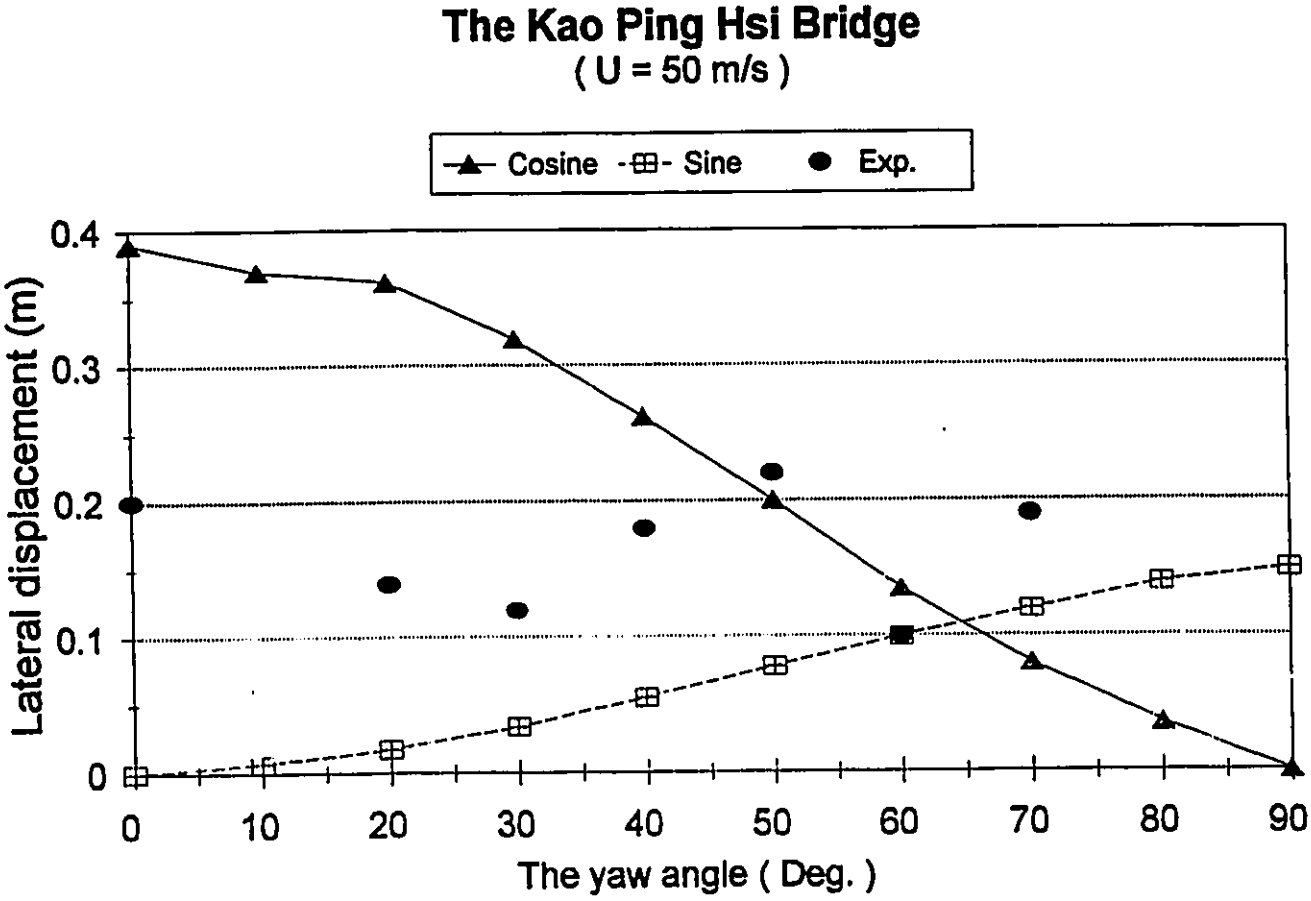

Fig. 3.25 Lateral deflection of main span free end vs. yaw angle (U = 50 m/s)

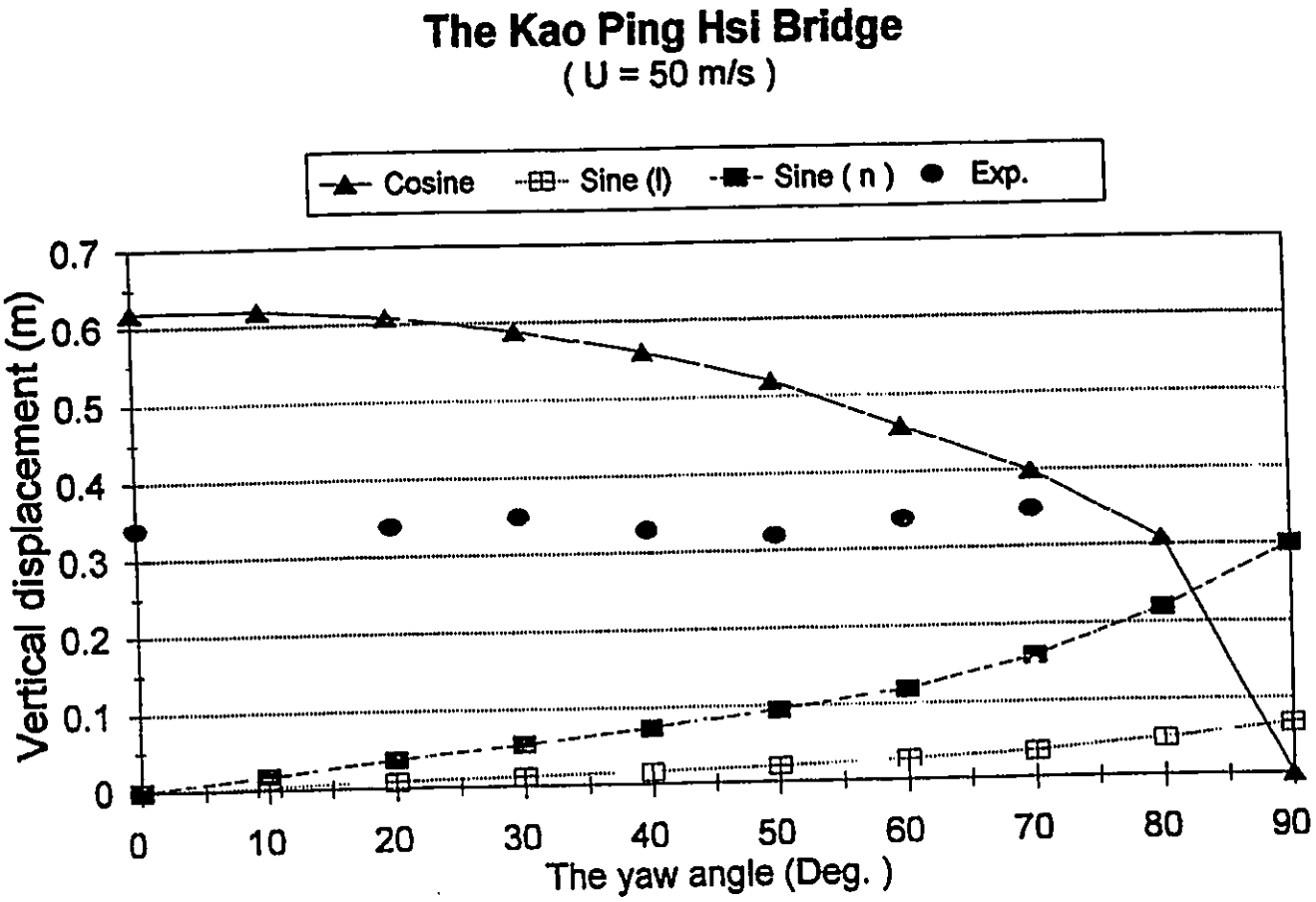

Fig. 3.26 Vertical deflection of main span free end vs. yaw angle (U=50 m/s)

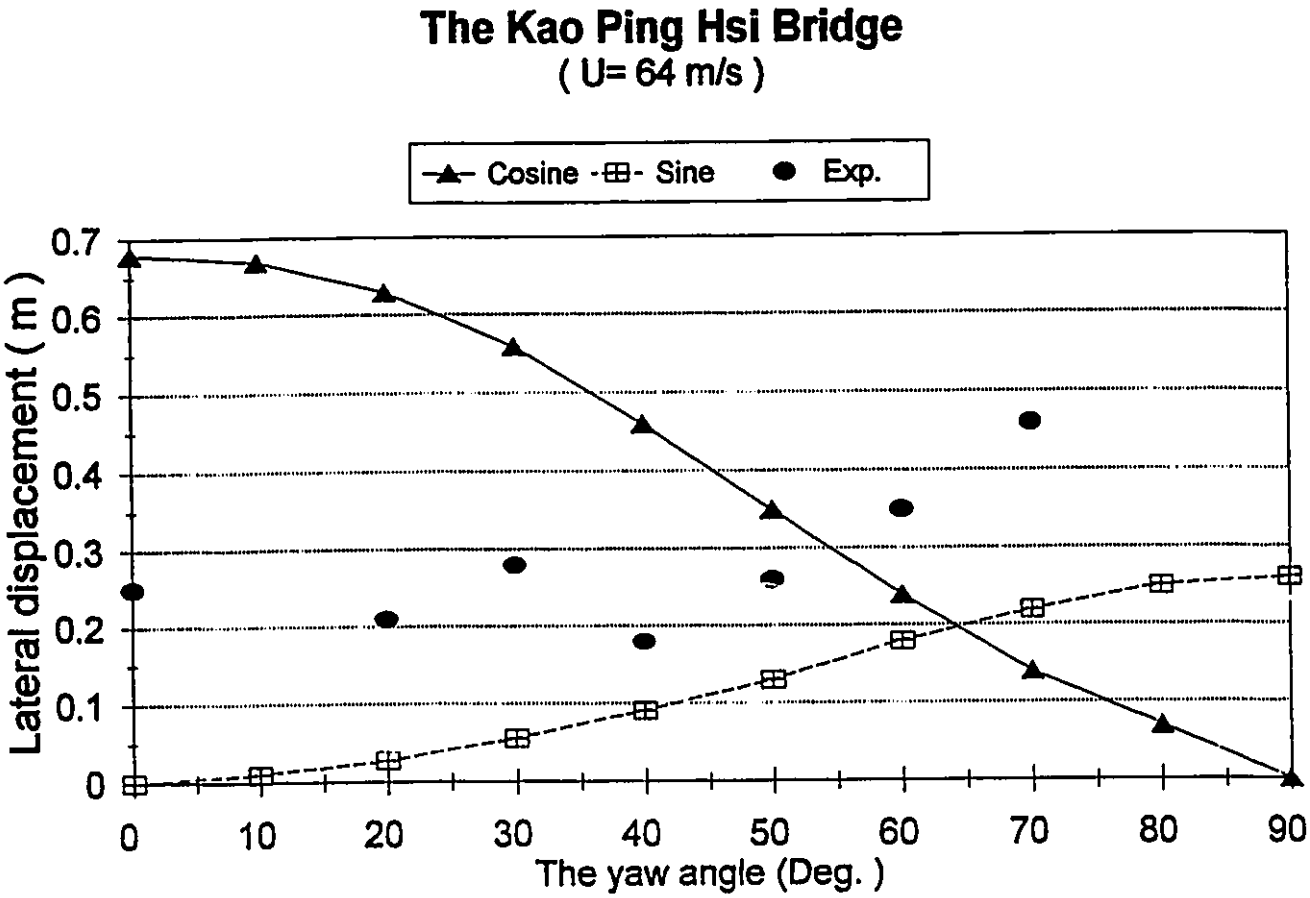

Fig. 3.27 Lateral deflection of main span free end vs. yaw angle (U=64 m/s)

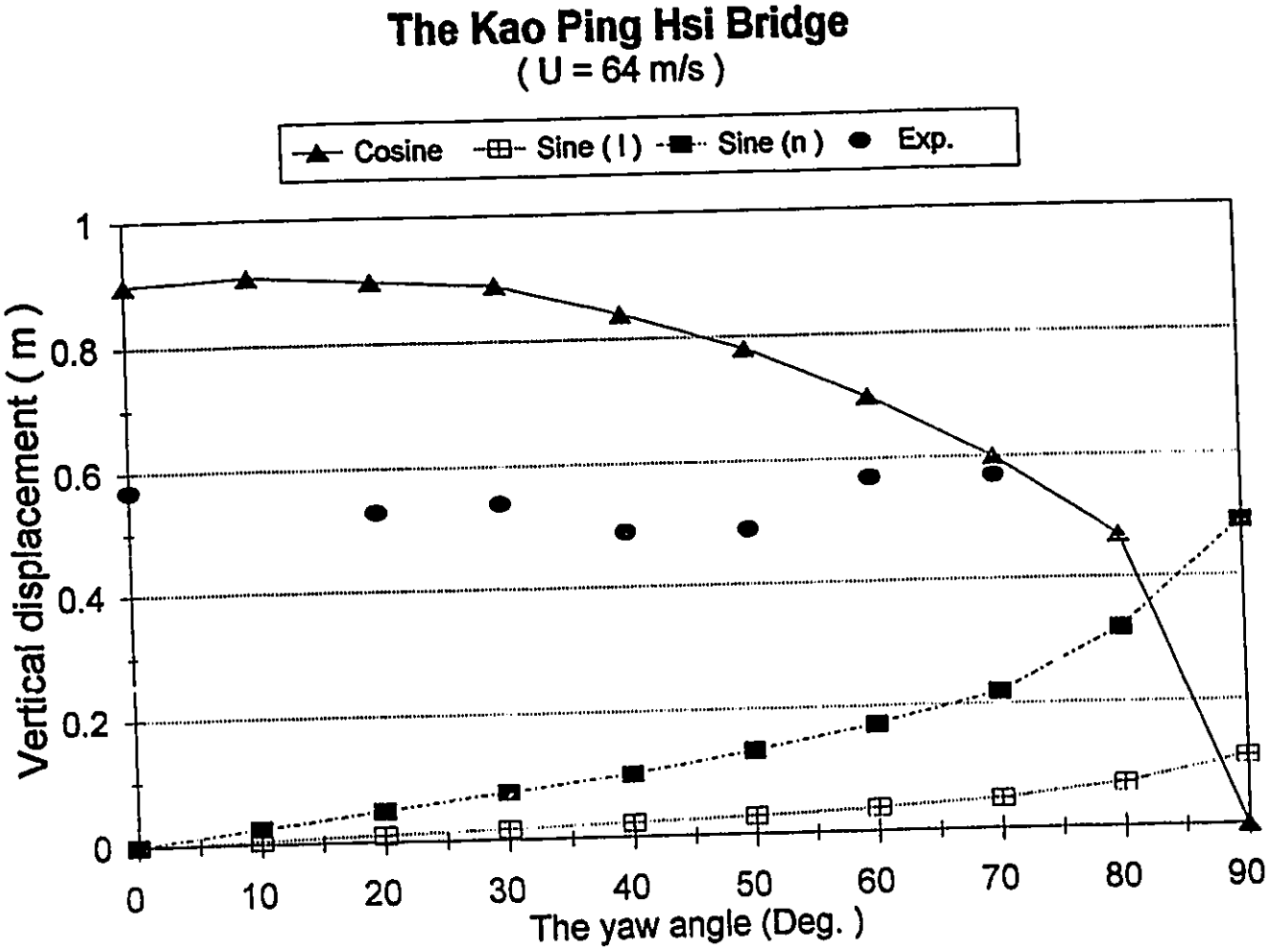

Fig. 3.28 Vertical deflection of main span free end vs. yaw angle (U=64 m/s)

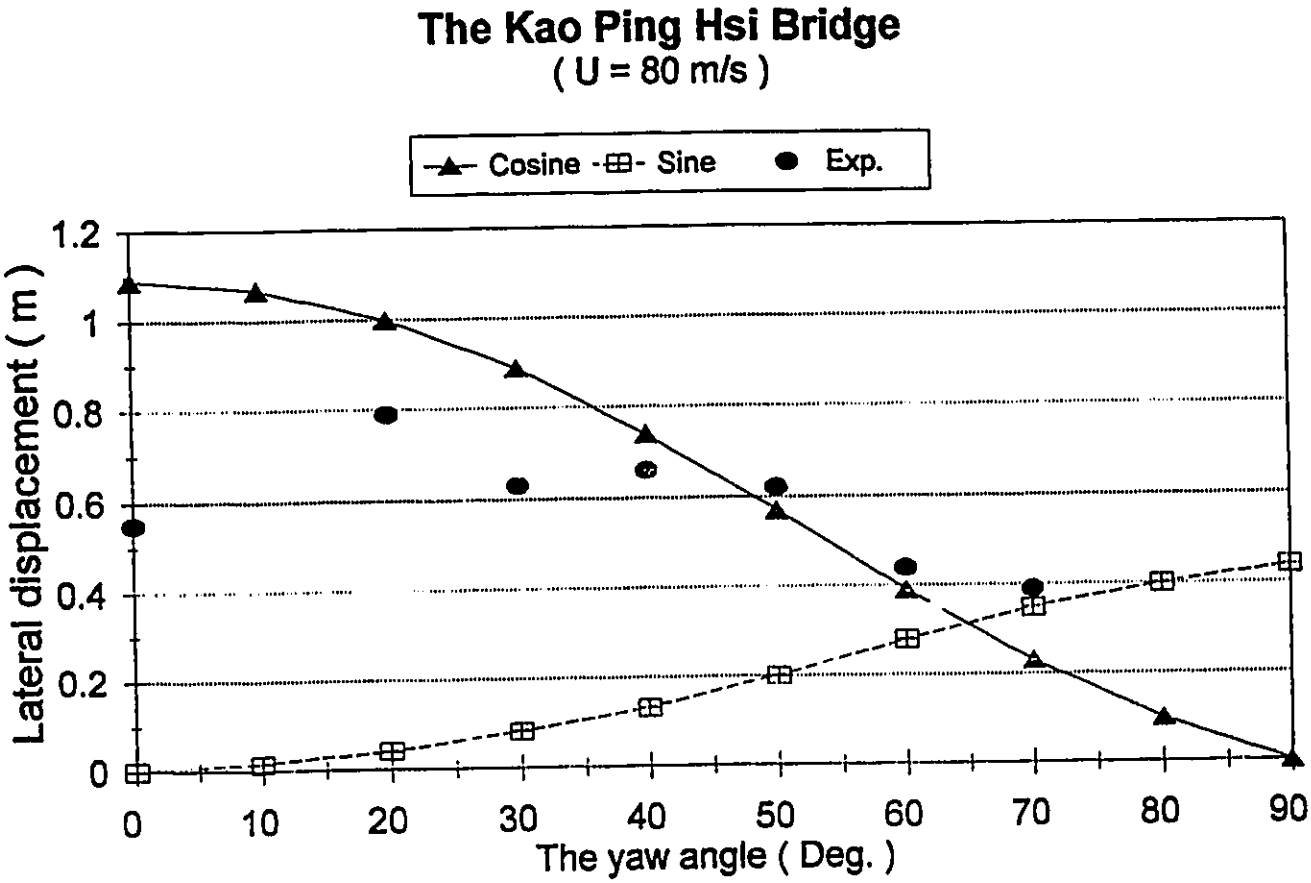

Fig. 3.29 Lateral deflection of main span free end vs. yaw angle (U=80 m/s)

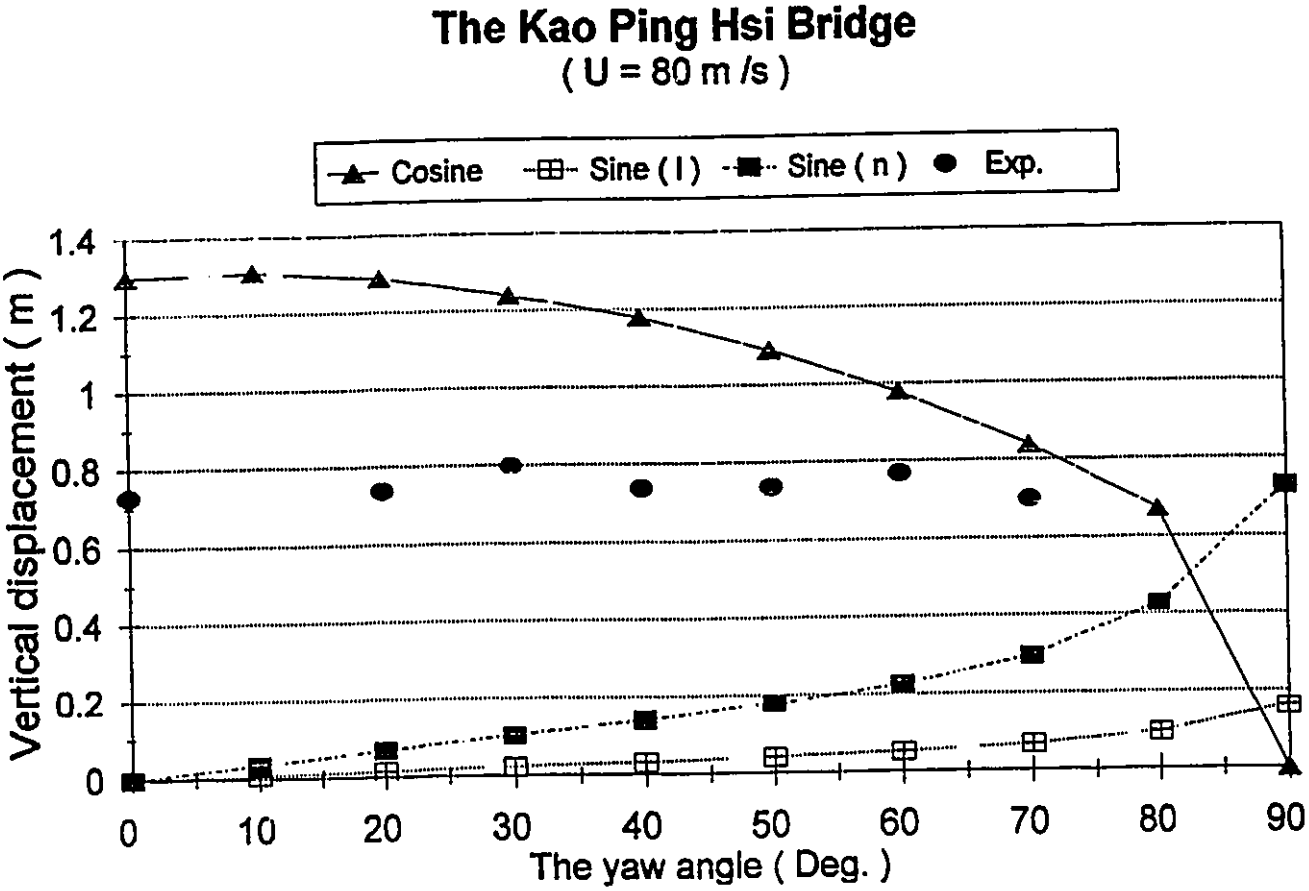

Fig. 3.30 Vertical deflection of main span free end vs. yaw angle (U=80 m/s)

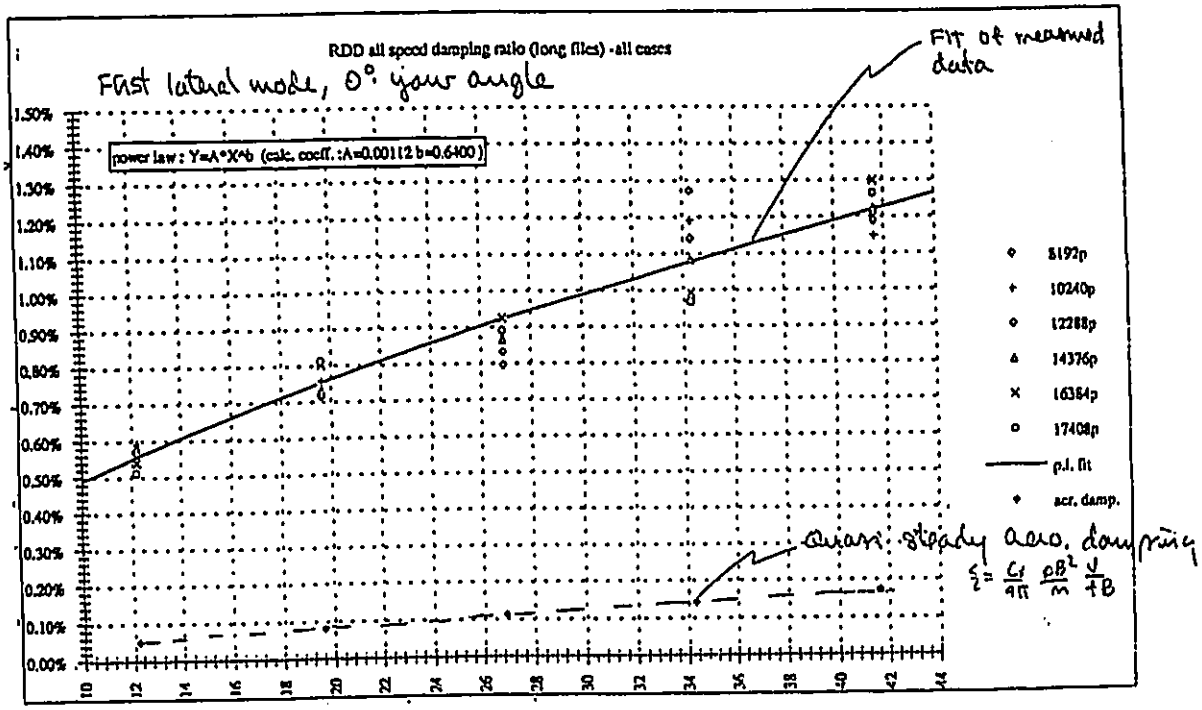

Fig. 4.1 Comparison of the measured damping and quasi-steady aerodynamic damping.